

**APPLICATION OF GUIDED WAVE FOR PIPELINE DEFECT  
IDENTIFICATION**

**POONG ZUI XIN**

**A project report submitted in partial fulfilment of the  
requirements for the award of Bachelor of Engineering  
(Honours) Mechanical Engineering**

**Lee Kong Chian Faculty of Engineering and Science  
Universiti Tunku Abdul Rahman**

**April 2019**

## DECLARATION

I hereby declare that this project report is based on my original work except for citations and quotations which have been duly acknowledged. I also declare that it has not been previously and concurrently submitted for any other degree or award at UTAR or other institutions.

Signature : \_\_\_\_\_

Name : POONG ZUI XIN  
\_\_\_\_\_

ID No. : 1504475  
\_\_\_\_\_

Date : \_\_\_\_\_

## APPROVAL FOR SUBMISSION

I certify that this project report entitled “**APPLICATION OF GUIDED WAVE FOR PIPELINE DEFECT IDENTIFICATION**” was prepared by **POONG ZUI XIN** has met the required standard for submission in partial fulfilment of the requirements for the award of Bachelor of **Bachelor of Engineering (Hons.) Mechanical Engineering** at Universiti Tunku Abdul Rahman.

Approved by,

Signature : \_\_\_\_\_

Supervisor : Prof. Dr. Andy Chit Tan  
\_\_\_\_\_

Date : \_\_\_\_\_

The copyright of this report belongs to the author under the terms of the copyright Act 1987 as qualified by Intellectual Property Policy of Universiti Tunku Abdul Rahman. Due acknowledgement shall always be made of the use of any material contained in, or derived from, this report.

© 2019, Poong Zui Xin. All right reserved.

## **ACKNOWLEDEMENTS**

First of all, I would like to express my gratitude to my final year project supervisor, Prof. Dr. Andy Chit Tan for his invaluable advice, guidance and his enormous patience throughout the development of the research. Also, thanks to my senior, master student Lee Wei Tang who involved in the pipeline project. With his experience and guidance, I was moving toward to correct direction and able to achieve aims and objectives.

In addition, I would also like to express my gratitude to my loving parents and friends who had helped and given me encouragement during the period of my research.

## **ABSTRACT**

In plant or factory, the use of pipeline system to deliver different kinds of fluids are very common. It is very important to check the health of pipeline regularly since failure and collapse of pipelines may cost millions or even human life. The main objective of this project is to detect the defect on the pipeline using Guided Wave. GW can be generated using different type of transducers that transform different kind of energy to mechanical stress. The selection of transducer is important to generate GW in a pipe, 3 common transducers use in GW generation are PZT, EMAT and magnetostrictive transducer. These transducers have their own pros and cons. In this study, magnetostrictive transducer is used to generate signal through the pipe. A further research was done in order to build GW actuator using magnetostrictive transducer. Due to the limitation of budget, nickel is chosen as the magnetostrictive material in this study and it is functioning well in this study.

In this report, a clear instruction of steps in data acquisition and experimental setup of test rig from sensors to result are shown. The design of GW actuator including the crucial components to build the actuator will be discussed in this study.

The model of GW actuator is built in this study according to the design mentioned. Programming software like MATLAB and LABVIEW is used in this study to write and generate desired signal and data acquisition.

Three sets of data are taken in this study. The first and second set is taken on a 1.5m long pipe with 6cm and 4 cm artificial defect respectively located at the middle of the pipe. The third set of data is taken at a 36m long pipe with few welded spot and pipe holder that will cause reflection of signal. A minimum propagate distance required to observe both wave modes was calculated and proved in this study.

## TABLE OF CONTENTS

<b>TABLE OF CONTENTS</b>	<b>vii</b>
<b>LIST OF TABLES</b>	<b>ix</b>
<b>LIST OF FIGURES</b>	<b>x</b>
<b>LIST OF SYMBOLS / ABBREVIATIONS</b>	<b>xii</b>

### CHAPTER

<b>1</b>	<b>INTRODUCTION</b>	<b>1</b>
	1.1 General Introduction	1
	1.2 Importance of the Study	2
	1.3 Problem Statement	2
	1.4 Aims and Objectives	2
	1.5 Scope and Limitation of the Study	3
<b>2</b>	<b>LITERATURE REVIEW</b>	<b>4</b>
	2.1 Introduction	4
	2.2 Literature Review	4
	2.3 Guided Wave	4
	2.4 Selection of Transducer	5
	2.4.1 Piezoelectric Transducer (PZT)	5
	2.4.2 Electromagnetic Transducer (EMAT)	5
	2.4.3 Magnetostrictive Transducer	6
	2.4.4 Comparative Analysis	6
	2.5 Magnetostiction	6
	2.5.1 Selection of Magnetostrictive Material	7
	2.6 Guided Wave Modes in Pipeline	8
	2.6.1 Dispersion Curve	9
	2.6.2 Guided Wave Mode Selection	10

2.6.3	Longitudinal Wave Generation Scheme	11
2.7	Summary	13
<b>3</b>	<b>METHODOLOGY AND WORK PLAN</b>	<b>14</b>
3.1	Introduction	14
3.2	Gantt Chart	15
3.3	Methodology	16
3.3.1	Function Generator	16
3.3.2	Amplifier	17
3.3.3	Guided Wave Signal Excitation	18
3.3.4	Data Acquisition	18
3.3.5	Signal Processing	21
3.3.6	Experimental Setup	21
<b>4</b>	<b>RESULTS AND DISCUSSIONS</b>	<b>23</b>
4.1	Introduction	23
4.2	Experimental Setup	23
4.3	Generated Signal	25
4.4	User Interface in Data Acquisition	25
4.5	Results Collected at Pipeline With 6cm Defect.	26
4.6	Results Collected at Pipeline With 4cm Defect.	29
4.7	Results Collected at 36m Pipeline	32
4.8	Summary	39
<b>5</b>	<b>CONCLUSIONS AND RECOMMENDATIONS</b>	<b>40</b>
5.1	Conclusions	40
5.2	Recommendations for Future Work	40
	<b>REFERENCES</b>	<b>42</b>



**LIST OF TABLES**

Table 2-1: Magnetostrictive Coefficient Values for Iron, Nickel and Cobalt.	7
Table 2-2: Signal Amplitude of Nickel and Iron Cobalt Transducer	8
Table 3-1: Gantt Chart for FYP 1	15
Table 3-2: Gantt Chart for FYP 2	15

## LIST OF FIGURES

Figure 2-1: Lining Up of Magnetic Domains In a Ferromagnetic Element by Joule Effect	7
Figure 2-2: Power Output of Nickel and Iron Cobalt Transducer (Vinogradov and Leonard, 2017)	8
Figure 2-3: Guided Wave Modes in pipe.	9
Figure 2-4: Dispersion Curve of Sample Pipe	10
Figure 2-5: Cylindrical Coordinate System ( $r\theta z$ ) of a Pipeline(Tribikram Kundu, 2004)	11
Figure 2-6: Oscillation Pattern of Longitudinal Guided Wave Mode.	12
Figure 3-1: Process Flow Chart	14
Figure 3-2: Flowchart of Methodology	16
Figure 3-3: National Instruments ELVIS	17
Figure 3-4: Amplifier	17
Figure 3-5: Guided Wave Excitation Design	18
Figure 3-6: Data Acquisition Steps	18
Figure 3-7: AE Sensor (SR40M) and Sensor Fixture	19
Figure 3-8: Preamplifier by Beijing Soundwel Technology Co. Ltd	19
Figure 3-9: Low Pass Filter (EF504)	20
Figure 3-10: Data Acquisition Module (NI-9223)	20
Figure 3-11: Code for Signal Generation	21
Figure 3-12: Design of Experimental Setup	22
Figure 4-1: Experimental Setup	23
Figure 4-2: Experimental Setup at Rooftop	24
Figure 4-3: GW Signal Generator	24

Figure 4-4: Signal with 60 kHz Frequency	25
Figure 4-5: Block Diagram in LABVIEW	25
Figure 4-6: User Interface of Data Acquisition	26
Figure 4-7: Location of Sensors at 6cm Defect Pipeline	26
Figure 4-8: Result on 6cm Defect Using 75 kHz Frequency	27
Figure 4-9: Result on 6cm Defect Using 60 kHz Frequency	27
Figure 4-10: Result on 6cm Defect Using 45 kHz Frequency	27
Figure 4-11: Result on 6cm Defect Using 30 kHz Frequency	28
Figure 4-12: Calculation Based on Result of 60 k Hz frequency	28
Figure 4-13: Wave Mode Velocity at 60kHz Frequency	29
Figure 4-14: Location of Sensors at 4cm Defect Pipeline	30
Figure 4-15: Result on 4cm Defect Using 75 kHz Frequency	30
Figure 4-16: Result on 4cm Defect Using 60 kHz Frequency	30
Figure 4-17: Result on 4cm Defect Using 45 kHz Frequency	31
Figure 4-18: Calculation Based on Result of 75 k Hz frequency	31
Figure 4-19: Wave Mode Velocity at 75kHz Frequency	32
Figure 4-20: Location of 36m Pipeline	34
Figure 4-21: Welded spot and Pipeline Holder	34
Figure 4-22: Distance between Sensor & Actuator: 60cm	35
Figure 4-23: Distance between Sensor & Actuator: 40cm	35
Figure 4-24: Distance between Sensor & Actuator: 20cm	36
Figure 4-25: Distance between Sensor & Actuator: 90cm	37
Figure 4-26: Distance between Sensor & Actuator: 110cm	38
Figure 4-27: Distance between Sensor & Actuator: 130cm	38

**LIST OF SYMBOLS / ABBREVIATIONS**

$\varepsilon$	Strain
$\sigma$	Externally applied stress
$H$	Externally applied magnetic field
$B$	Magnetic induction
$\mu^\sigma$	Permeability at constant stress
$E_y$	Young's modulus at constant applied magnetic field
$\mu_0$	Permeability of air
$N_c$	Number of turns of coil
$I$	Externally applied current
$L_c$	Length of coil
GW	Guided Wave
NDE	Non-Destructive Evaluation
NDT	Non-Destructive Testing
PZT	Piezoelectric Transducer
EMAT	Electromagnetic Acoustic Transducer
FFT	Fast Fourier Transform
AE	Acoustic Emission
ADC	Analog Digital Conversion

## CHAPTER 1

### INTRODUCTION

#### 1.1 General Introduction

In plant or factory, the use of pipeline system to deliver different kinds of fluids are very common. It is very important to check the health of pipeline regularly since failure and collapse of pipelines may cost millions or even human life. There have been a few methods to perform inspection on the health of the pipelines non-destructively. The application of Guided Wave (GW) for elongated structure inspection is one of the latest strategies in the field of Non-Destructive Evaluation (NDE) also called Non-Destructive Testing (NDT). The name GW comes from its fundamental principle, the method produce waves using transducer that transfer along the long-range structure while guided by its boundaries. One of the characteristic of this method is allowing the wave to travel a long range with little loss of energy. When the propagated waves hit a defect like corrosion or leakage, a reflected wave will be detected by a sensor. This technique allows determining the location or quantity of the defect along the elongated structure.

In this study, GW is used to identify the defect of the pipeline. GW can be generated using different type of transducers that transform different kind of energy to mechanical stress. Besides that, few types of GW modes like longitudinal, torsional and flexural also have different characteristic in application of inspection. Transducer construction method also will be different when need to generate different wave mode. All of these factors will be further discussed in chapter 2.

Raw data obtained can be analysed in time and frequency domain. This can be done by using the software MATLAB. Location of defect can be detected by studying the graph of propagated guided wave, when the wave is reflected by the barrier formed by the defect. The amplitude of the propagating wave also will be affected by the quantity of the defects throughout the whole pipeline.

## **1.2 Importance of the Study**

The use of pipeline system to deliver different kinds of fluids is very common in a plant or factory. Failure or collapse of pipeline may cost million or even human life. Thus, it is very important to check the condition of the structure regularly.

The importance of this study is to construct hardware and software for pipeline defect identification using application of Guided Wave. GW can be produced using different transducer for example like piezoelectric transducer (PZT), magnetostrictive transducer and electromagnetic acoustic transducer (EMAT). These transducers are going to be investigated in this study.

Collected data can be analysed in time domain and frequency domain. These can be done by using the software MATLAB. Time domain gives information to determine the location of defect but not very sensitive to quantity of defect. In order to determine quantity of defect, data have to be analysed in frequency domain. Fourier Series can be used to transform time domain to frequency domain. This also can be done by using the Fast Fourier Transform (FFT) function in MATLAB.

GW is mainly used in elongated structure health inspection. It can propagate in a long distance with a little loss of energy. Engineers can use this method in elongated structure inspection to determine the location of the defect.

## **1.3 Problem Statement**

Pipeline inspection is very important because pipeline failure may cause millions or even human. But underground pipeline inspection is not an easy task. Digging is one of the most tedious, expensive, harmful and invasive parts in underground pipeline inspection. Both machine and manual digging require a large amount of money and will also cause the destruction of land or property, even if you don't find a problem in the pipeline after all these affords.

## **1.4 Aims and Objectives**

The aim of this study is to detect a pipeline defect by using the application Guided Wave. The objectives of this study consists the following:

- Detection of pipeline defect with Guided Wave.
- Conduct the experiment test rig to simulate signal for pipeline defect identification.

## 1.5 Scope and Limitation of the Study

In order to achieve the aims and objectives, student designed some scopes that able to reach to goal. The scopes of this study include the following:

- Design own methodology and test rig to identify defect of pipeline based on application of Guided Wave.
- Galvanised iron Class B 3 inches diameter with 1.5m long will be used for the test rig.
- Use MATLAB and LABVIEW for data acquisition and further signal processing like time domain to frequency domain transformation.

However, the limitation of this study may consist of the following:

- The cost of a better magnetostrictive material like iron cobalt is high, an alternative material, nickel which is much cheaper may use in this experiment. However, the signal produced also 5 to 10 times lower compare with iron cobalt.
- In order to build a complete hardware of Guided Wave, it should be consist of wave generation and signal acquisition. However, wave generation will be focused in this study; signal collection using Guided Wave is expected to be continued in future. Acoustic emission (AE) sensor is used in this research to replace Guided Wave based sensor.

## CHAPTER 2

### LITERATURE REVIEW

#### 2.1 Introduction

This chapter will focus on the research of Guided Wave on elongated structure. Beside, some research on MATLAB had been done to better understand how to carry out signal processing.

#### 2.2 Literature Review

The literature review will focus on the transducer type, magnetostrictive material and guided wave modes.

#### 2.3 Guided Wave

The application of Guided Wave (GW) for elongated structure inspection is one of the latest strategies in the field of Non-Destructive Evaluation (NDE) also called Non-Destructive Testing (NDT)(Liu *et al.*, 2010). The name GW comes from its fundamental principle, the method produce waves using transducer that transfer along the long-range structure while guided by its boundaries. The benefits using Guided Wave for pipeline inspection include:

- Large section of pipeline can be inspected from a single probe position
- Inspection can be carried out without moving the pipe thus avoiding potential leaks and protecting the environment
- Cost effectiveness because of inspection simplicity and speed
- Ability to determine location and quantity of the defect on the pipe
- Inspection can be carried out without removing the coating or insulation on the pipe except the location of the transducer tools

Guided Wave can be produced using different transducer piezoelectric transducer (PZT), magnetostrictive transducer and electromagnetic acoustic transducer (EMAT). Different wave modes such as longitudinal, torsional and flexural modes can be produced. Details will be further discussed in this study.



## **2.4 Selection of Transducer**

There are different ways of generating GW for pipeline inspection. The main difference these ways are which type of transducer is being used. Currently, type transducers used in application of Guided Wave for pipeline inspection are transducer piezoelectric transducer (PZT), magnetostrictive transducer and electromagnetic acoustic transducer (EMAT).

### **2.4.1 Piezoelectric Transducer (PZT)**

Guided Wave generation by PZT is a very common method in inspection application (Schaal *et al.*, 2014). PZT is a type of electroacoustic transducer that works based on the effect of piezoelectric, it converts energy between electric energy and mechanical energy. When an electric field is activated, the piezoelectric material will produce mechanical wave. Inversely, when mechanical stress or strain is applied on piezoelectric material, it will produce electric charge. From (Khaligh, Zeng and Zheng, 2010), piezoelectric materials commonly used include piezoelectric ceramic, piezoelectric composite material, and piezoelectric crystals. The mechanical waves generated by piezoelectric material are propagated to the elongated structure through a coupling or bonding medium. Therefore, the condition of coupling medium will has a close response with the transducer's performance. In order to generate GW with PZT, numbers of PZT have to form an array around the pipeline structure, each of them are connected in series. This method is quite costly due to the numbers of PZT.

### **2.4.2 Electromagnetic Transducer (EMAT)**

EMAT are used in Non-Destructive Testing field due to one of its capability which is able to detect or generate ultrasonic wave in conductive or ferromagnetic component without any coupling or bonding medium. This is very useful since it doesn't need to remove coating on the sample to perform inspection. The mechanical vibration is generated based on theory of Lorentz force or magnetostictive effect. The EMAT generally consists of components like a coil, a magnet and conductive or ferromagnetic components. Different waves mode can be generated by different configuration of setup (Chimenti, 2014). Low strength of the EMAT produced signal is a main advantage of this method.

### 2.4.3 Magnetostrictive Transducer

The use of magnetostrictive transducer has been widely utilized in Non-Destructive Testing. Specifically in generation and acquisition of GW in inspection of elongated structure such as pipeline (Paper and Vinogradov, 2009; Kim and Kwon, 2015). Magnetostrictive transducer is a type of transducer that works based on the principle of Villari and Joule effect (Tatarinov *et al.*, 2018). It required a magnetostrictive material like nickel or iron cobalt. The main idea is the dimension of the material will changed when magnetic field is applied on it, Vice Versa. In order to generate GW using magnetostrictive transducer, a magnetostrictive strip has to wrap around the sample at a single location, a coil have to wound around the magnetostictive strip, an alternating current is provided to the coil and create an alternative changing of magnetic field and cause changing of dimension of the strip then create vibration.

### 2.4.4 Comparative Analysis

These three transducers have their own pros and cons. PZT has the advantage of higher rate of energy conversion(Luo *et al.*, 2018). However, its performance will be highly affected by the coupling or bonding medium. EMAT can solve the coupling medium problem since EMAT does not required physical contact to perform inspection. However, its low strength of signal is not suitable for long ranged pipeline inspection. Magnetostictive transducer has more advantages compare with the other two transducers. Its components are cheap, it also allows inspection on non-ferrous pipe materials and it can provide a uniform circumferential vibration while piezoelectric collar provides segmented excitations. Magnetostictive transducer is chose to generate guided wave for this study.

## 2.5 Magnetostiction

Magnetostiction was an effect first identified by James Joule in 1842 during observing a sample of iron(Joule, 1847) and being widely known as Joule Effect. It is a phenomenon that causes a ferromagnetic element change their shape and dimension when magnetic field is applied on it. Ferromagnetic elements having an internal structure named magnetic domain, they organized in regions of uniform magnetic polarization. Magnetic domains rotate and line up themselves when an external magnetic field is applied and produce a shape change as shown in Figure 1.

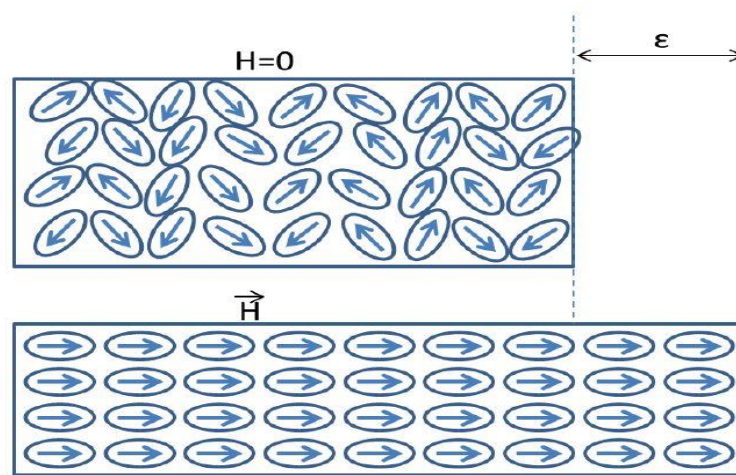


Figure 2-1: Lining Up of Magnetic Domains In a Ferromagnetic Element by Joule Effect

### 2.5.1 Selection of Magnetostrictive Material

Pure elements with magnetostriction effect include cobalt, iron and nickel. Alloy that contains any one of them also will exhibit magnetostriction. The degree of magnetostriction can be quantified by the magnetostriction coefficient,  $\lambda$ , which may be positive or negative. It defined as the fraction changed in length also called as strain ratio to the magnetization of the material. Negative magnetostriction material will contract when magnetic field is applied, Vice Versa. In the table below, magnetostrictive coefficient of cobalt, iron and nickel with different anisotropy is shown in table below. The values were gathered experimentally by (Myers, 1997).

Table 2-1: Magnetostrictive Coefficient Values for Iron, Nickel and Cobalt.

Material	Crystal Axis	Magnetostriction Coefficient, $\lambda$ ( $\times 10^{-5}$ ) ((m/m)/(A/m))
Fe	100	+(1.1 - 2.0)
Fe	111	-(1.3 - 2.0)
Fe	polycrystal	-0.8
Ni	100	-(5.0 - 5.2)
Ni	111	-2.7
Ni	polycrystal	-(2.5 - 4.7)
Co	polycrystal	-(5.0 - 6.0)

According to articles from (Bertoncini *et al.*, 2016) and (Vinogradov and Leonard, 2017), show that iron cobalt alloy has a better result for a magnetostrictive transducer. It has a higher sensitivity and power output for detection and long range inspection. Iron cobalt transducer is a good choice when considering long term or long range inspection. After student look into market, the price of iron cobalt strip is out of available budget when just need to purchase a low quantity like 1kg. Nickel strip is an alternate choice due to this limitation. Figure 2 and table 2 below show the comparison between nickel and iron cobalt transducer(Bertoncini *et al.*, 2016).

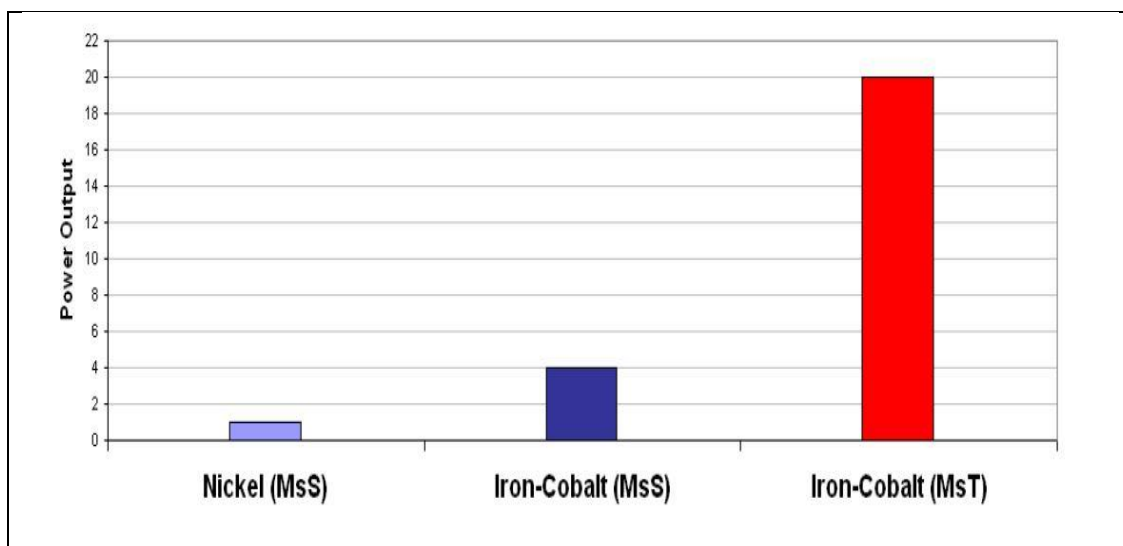


Figure 2-2: Power Output of Nickel and Iron Cobalt Transducer (Vinogradov and Leonard, 2017)

Table 2-2: Signal Amplitude of Nickel and Iron Cobalt Transducer

Transducer	Signal Amplitude(V)	Signal to Noise Ratio
Nickel	0.12	29dB
Iron Cobalt	1.25	32dB

## 2.6 Guided Wave Modes in Pipeline

There are many guided wave modes in plates and pipes. These modes are known as symmetric wave modes and asymmetric wave modes. Symmetric wave modes include longitudinal and torsional while asymmetric wave modes also known as flexural wave mode. Figure 2.3 below shows these 3 modes(Wang *et al.*, 2016). To distinguish the longitudinal, torsional and flexural modes from each other, letters L,

T and F are given respectively follow with a suffix contains 2 numbers. The first number indicates wave order while the second indicates its harmonic.

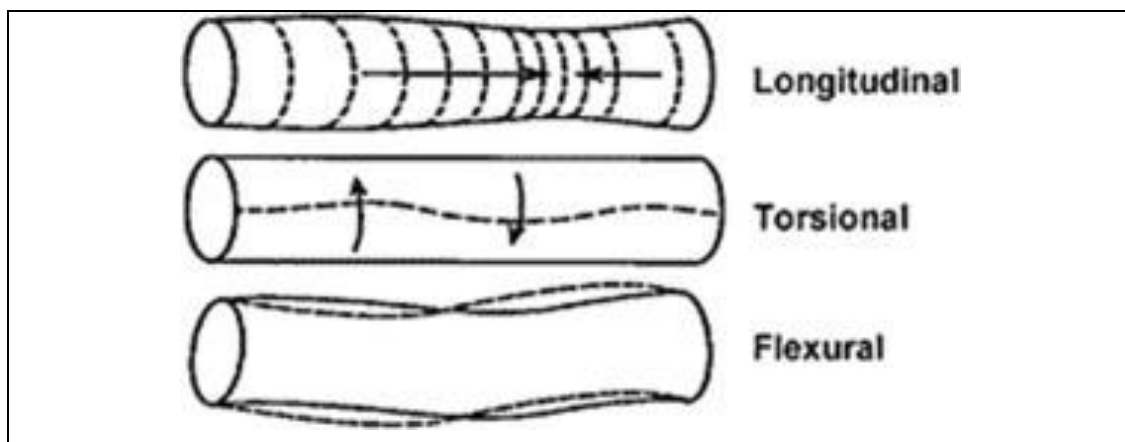


Figure 2-3: Guided Wave Modes in pipe.

### 2.6.1 Dispersion Curve

These waves propagate at different velocities and they are dispersive, also can be said that their velocity is a function of frequency (Panda *et al.*, 2012). The dispersion curve of the galvanized iron pipe with 89.5mm outer diameter and 4mm thickness use in this study was calculated and plotted using PCdisp MATLAB function. The dispersion curve is shown in figure 4 below. The dispersion curve shows a number of important characteristics. Firstly, it shows the number of modes increases as the frequency increases. Secondly, each mode is very dispersive at low frequency. Thirdly, torsional wave mode is not dispersive at every frequency, which makes it a very attractive choice for inspection.

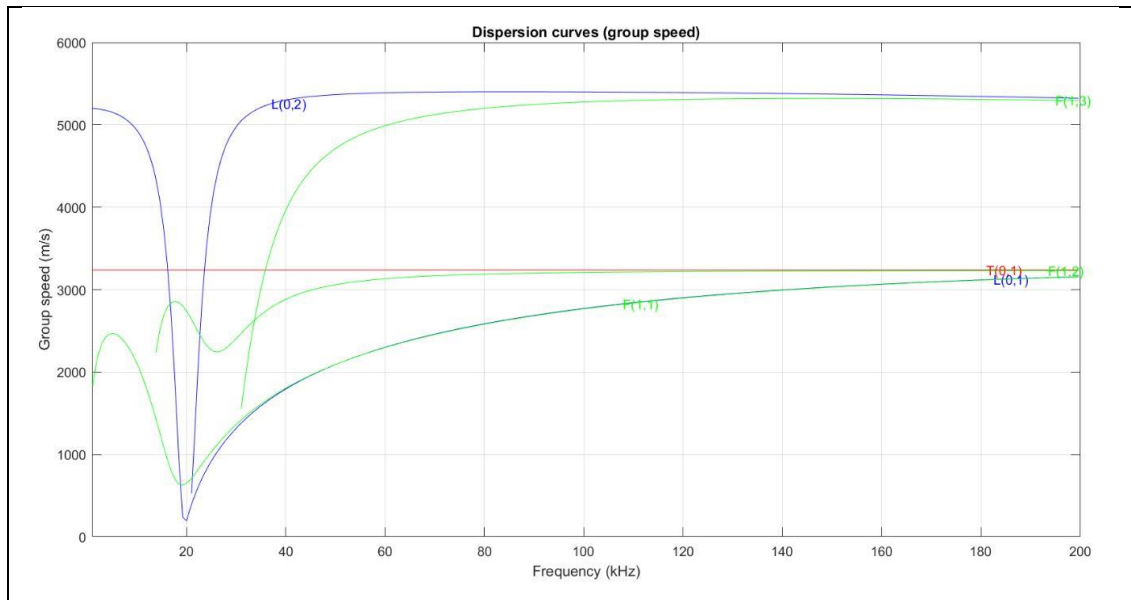


Figure 2-4: Dispersion Curve of Sample Pipe

### 2.6.2 Guided Wave Mode Selection

The  $T(0, 1)$  and  $L(0, 2)$  are the most attractive modes to generate in most application of inspection (Alleyne, Vogt and Cawley, 2009). This because the  $T(0, 1)$  wave mode is not dispersive at all range of frequency (Kim *et al.*, 2005) while  $L(0, 2)$  wave mode is not dispersive for a wide range of frequency. Flexural wave mode is not commonly used because of it is very dispersive and low sensitivity (Furusawa, Kojima and Morikawa, 2015), (Tatarinov *et al.*, 2018).

Besides that, the longitudinal wave mode consists radial displacement,  $r$  axis and axial displacement,  $z$  axis, while the torsional wave mode consist only circumferential displacement,  $\theta$  axis. These axes are shown in figure 2.5. However, the AE sensors going to use in this study is more sensitive to radial displacement. With these reasons, the wave mode student is going to use in this study is longitudinal wave mode.

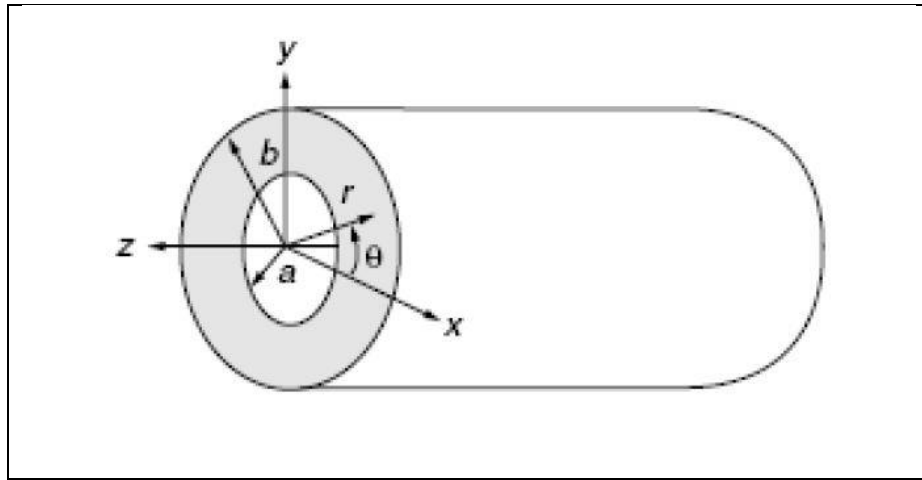


Figure 2-5: Cylindrical Coordinate System ( $r\theta z$ ) of a Pipeline (Tribikram Kundu, 2004)

### 2.6.3 Longitudinal Wave Generation Scheme

In order to excite different guided wave modes require different experiment setup method. In this study, longitudinal wave mode is chosen. For this wave mode, the propagation of the wave is parallel to the displacement of medium. The oscillation pattern is shown in figure 2.6. The dimension of pipe in  $r$  axis is very small compare with its  $z$  axis. Therefore, the propagated wave can be considered as a 1-D stress wave. This 1-D magnetostrictive process can be represented by 2 coupled equations below (Zhang *et al.*, 2014), (FT Calkins, 2006).

$$\varepsilon = \sigma/E_y + \partial\varepsilon/\partial H|\sigma \cdot H \quad (2.1)$$

$$B = \partial B/\partial\sigma|_H \cdot \sigma + \mu^\sigma H \quad (2.2)$$

Where

- $\varepsilon$  Strain;
- $\sigma$  Externally applied stress;
- $H$  Externally applied magnetic field;
- $B$  Magnetic induction;
- $\mu^\sigma$  Permeability at constant stress;
- $E_y$  Young's modulus at constant applied magnetic field.

In this study, an alternating current is transmitted in the coil to produce alternating magnetic field strength for this magnetostrictive transducer by the

fundamental of Lenz's law. The electromagnetic relationship can be simply described as

$$B = \mu_0 N_c I / L_c \quad (2.3)$$

Where

- $\mu_0$  Permeability of air;
- $N_c$  Number of turns of coil;
- $I$  Externally applied current;
- $L_c$  Length of coil.

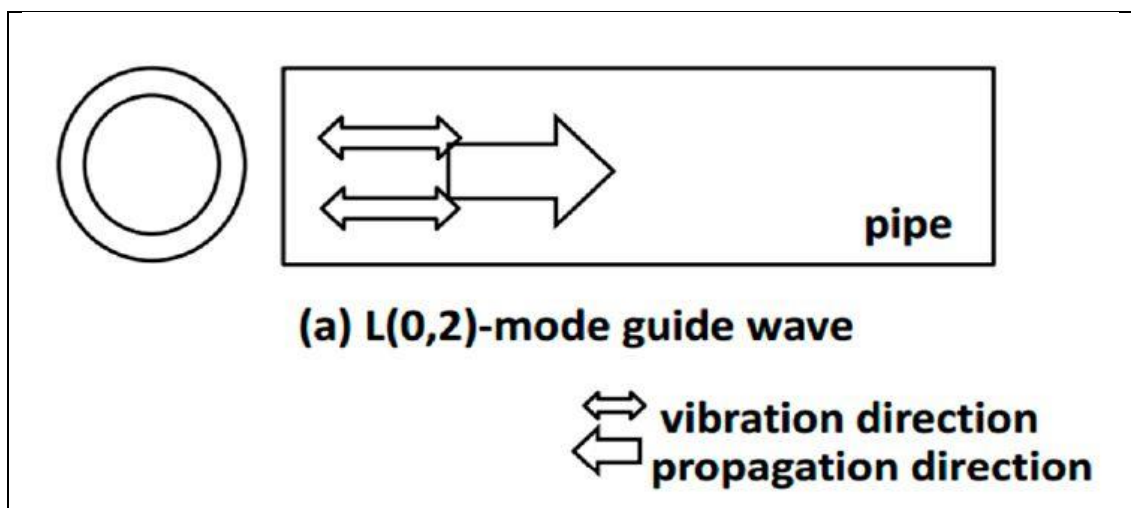


Figure 2-6: Oscillation Pattern of Longitudinal Guided Wave Mode.

## 2.7 Background Noise

Background noise is basically the unwanted signal. Background noise includes extrinsic noise and intrinsic noise. Extrinsic noise is the noise obtained from the external source while intrinsic noise is majorly found in the electronic circuit. In pipeline health inspection field, extrinsic noises are normally produced by pump or compressor that working with the pipe.

Background noise cannot be avoided because it is caused by the electromagnetic field, the turbulence flow and the data acquisition component that use to record data. The background noise can be cancelled using noise cancellation technique like cross-correlation and wavelet transform. These background noises may cause false detection of defect. Therefore, signal processing is important to



cancel background noise. The reflected signal and background noise can be determined by analysing the characteristics of time domain and frequency domain.

## **2.8 Summary**

In the first part this chapter, the type of transducers to generate GW is discussed. 3 types of transducers are compared and the final decision is magnetostrictive transducer.

Although cobalt iron is a better magnetostrictive material to build a magnetostrictive transducer, nickel is chosen as a magnetostrictive material that going to be used in this study after some considerations mentioned above.

After that, 3 type of GW wave modes are analysed and longitudinal wave mode is chosen due to its dispersion characteristic and sensor available in lab.

To generate longitudinal mode using GW method, 3 crucial components are nickel strip, copper wire and magnet. The nickel strip with length follow the pipe's diameter should be positioned at the end of the pipe. The copper wire with 90m long has to wound around the nickel strip to provide alternating magnetic field to change the dimension of the nickel. Magnets have to position at the 2 sides of the nickel strip to provide bias magnetic field to control the mode of vibration.

## CHAPTER 3

### METHODOLOGY AND WORK PLAN

#### 3.1 Introduction

This chapter will discuss about the methodology and work plan of this project. Based on the literatures reviewed in previous chapter, the info obtained will be used to design GW excitation method for pipeline defect identification. Figure 3.1 shows the process flow chart of this project.

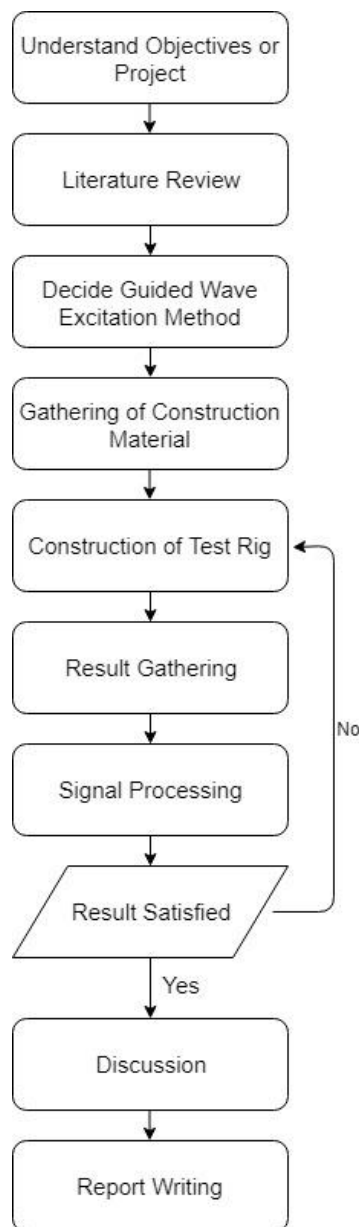


Figure 3-1: Process Flow Chart

### 3.2 Gantt Chart

In order to complete this project in 2 semester time, project is break into smaller tasks so that it is easier to track of progress and key dates. Table 3.1 and table 3.2 show the Gantt Chart of FYP 1 and FYP 2.

Table 3-1: Gantt Chart for FYP 1

No.	Project Activities	W1	W2	W3	W4	W5	W6	W7	W8	W9	W10	W11	W12	W13	W14
M1	Project formulation and Project planning														
M2	Literature Review														
M3	Data Gathering														
M4	Report Writing and Presentation														

Table 3-2: Gantt Chart for FYP 2

No.	Project Activities	W1	W2	W3	W4	W5	W6	W7	W8	W9	W10	W11	W12	W13	W14
M1	Material Gathering														
M2	Construction of Test Rig														
M3	Data Gathering														
M4	Report Writing and Presentation														

### 3.3 Methodology

The methodology of this study can be split into 4 major steps before obtaining experiment result. Figure 3.2 shows these major steps. Description of these steps will be further discussed in this chapter.

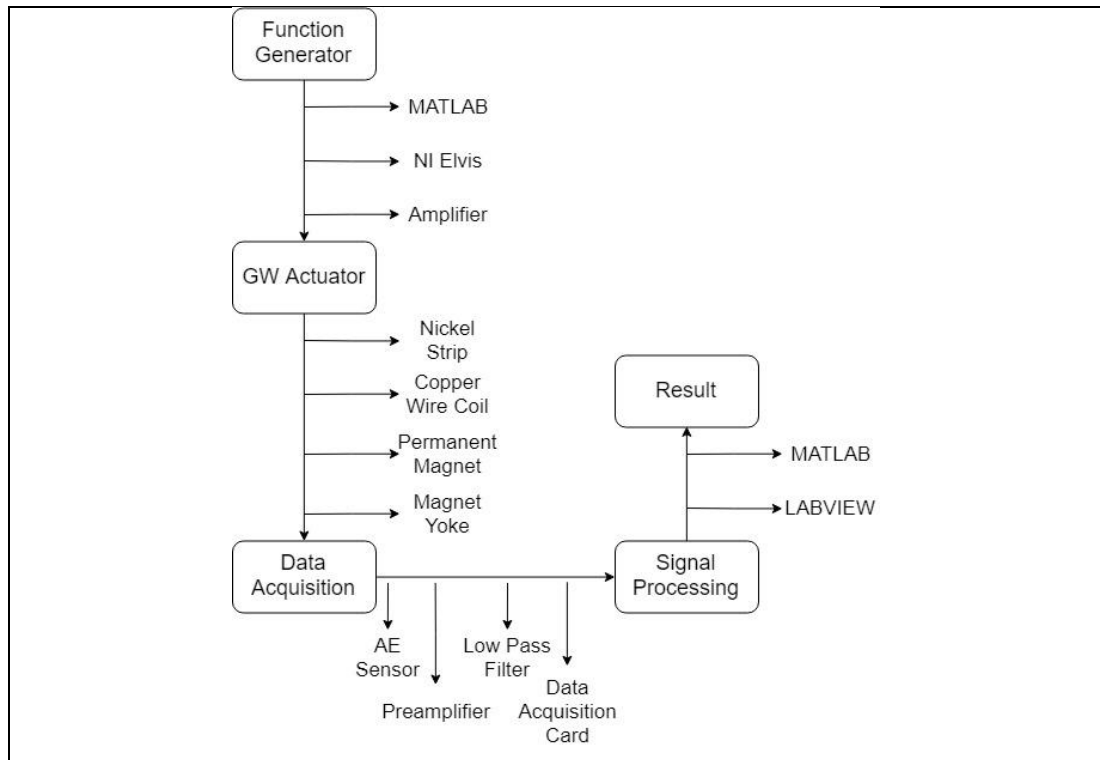


Figure 3-2: Flowchart of Methodology

#### 3.3.1 Function Generator

From previous chapter, we know that magnetostrictive material requires an alternating magnetic field to produce mechanical vibration, an alternating magnetic field can be produced by an alternating current passing through a coil by Lenz's Law. National Instruments ELVIS shown in figure 3.3 is a device that including some common lab instruments such as oscilloscope, function generator, multimeter etc. This device will do its job as an alternating current generator in this step.

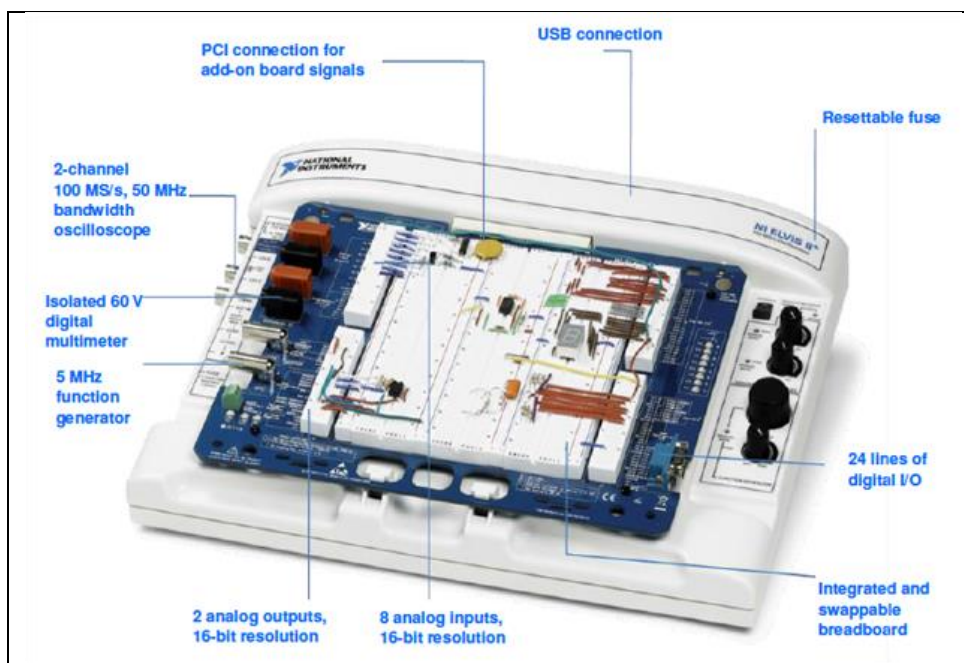


Figure 3-3: National Instruments ELVIS

### 3.3.2 Amplifier

The maximum output current from the NI ELVIS is only 0.5mA, which is not enough to generate high alternating magnetic field. An amplifier is used to amplify the signal generated from NI ELVIS

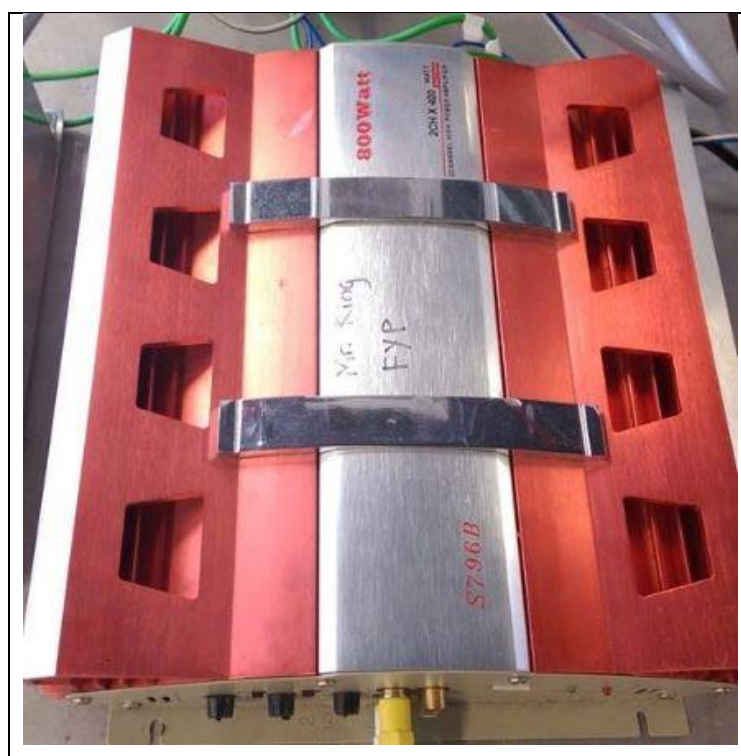


Figure 3-4: Amplifier

### 3.3.3 Guided Wave Signal Excitation

The main components of GW signal generator are shown in figure 3.5, it includes:

- Nickel Strip: It transforms alternating magnetic field into mechanical stress with its magnetostriction characteristic.
- Coil: It provides alternating magnetic field.
- Permanent Magnet: It provides bias magnetic field to strains the material that the guided wave is propagated in longitudinal mode.
- Yoke: It holds the position of the permanent magnet.

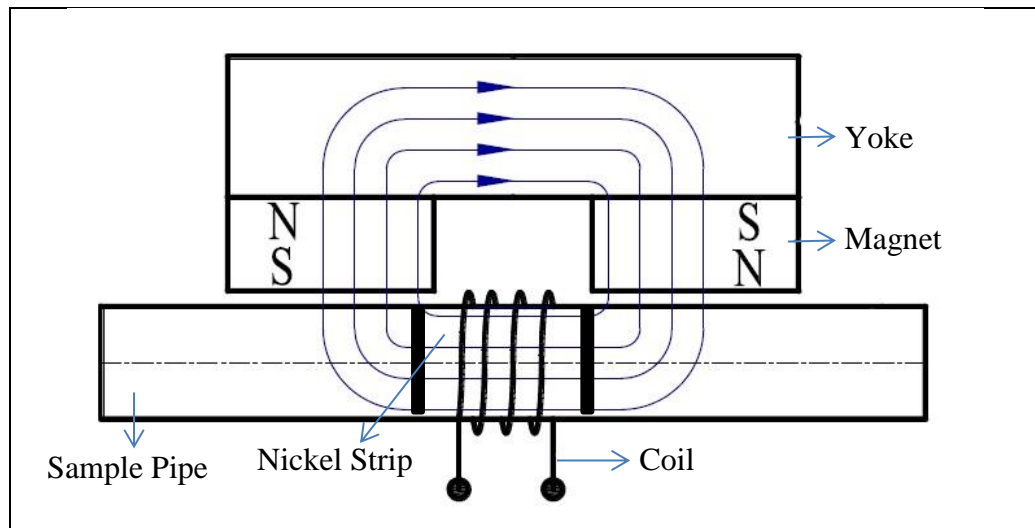


Figure 3-5: Guided Wave Excitation Design

### 3.3.4 Data Acquisition

The steps of data acquisition for this study are shown in figure 3.6 below. Vibration signals have to pass through few devices before being saved into a computer for further signal processing.

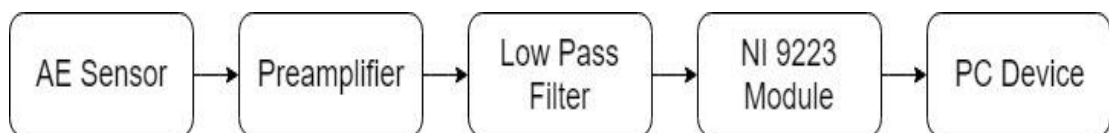


Figure 3-6: Data Acquisition Steps

### 3.3.4.1 AE Sensor

AE sensor will be used as vibration pickup in this study. The model of this AE sensor is SR40M by Beijing Soundwel Technology Co. Ltd with the frequency range of 15kHz to 70kHz, which is mainly used in leak detection. A magnetic sensor holder will be used to fix the position of the sensor.



Figure 3-7: AE Sensor (SR40M) and Sensor Fixture

### 3.3.4.2 Preamplifier

A preamplifier will be used to amplify the signal picked up from AE sensor with a gain of 40dB under single-ended mode before it connects with the data acquisition module.



Figure 3-8: Preamplifier by Beijing Soundwel Technology Co. Ltd

### 3.3.4.3 Low Pass Filter

Aliasing problem will occur when the sampling rate is not at least double of the detected frequency (Nyquist frequency). A low pass filter with  $\leq 240$  kHz passband by THORLABS will be connected between preamplifier and data acquisition module to filter unwanted signal and noise. It is a passive filter, therefore no power input is required. It acts as an anti-aliasing filter which prevents the aliasing components from being sampled.



Figure 3-9: Low Pass Filter (EF504)

### 3.3.4.4 Data Acquisition Module

Data acquisition module NI 9223 from National Instruments will be used to perform data acquisition in this study. Its function is converts analog value from sensor to digital value to computer devices (ADC). Its maximum sampling rate is 1MS/s/CH(1 Mega sample per second per channel).



Figure 3-10: Data Acquisition Module (NI-9223)



### 3.3.5 Signal Processing

A code is written in MATLAB, this code is to generate a 5 cycles wave with different frequencies. After running this code, a wave will be plotted and saved in txt format. A National Instrument driver, NI DAQmx will be used to convert the txt format in to wdt format to make it readable by NI Elvis.

```

clc
close all
clear

% Pulse generation
Fs = 2e6; %Sampling Rate
fc = 30e3; % Frequency of Pulse
cycl = 5; % number of cycles

tp = 1/fc*cycl; % time length of pulse
tsig = tp;% 4e-3; %tp;% total signal length
Ns = round(Fs*tp);
t = [0:Ns-1]'/Fs;
x = sin(2*pi*fc*t).*hann(Ns);

% zero padding
% tpad = round((tsig-max(t))*Fs);
% x = padarray(x,[round(tpad/15) 0],'pre');
% x = padarray(x,[tpad-round(tpad/15) 0],'post');
% figure; plot([0:length(x)-1]*Fs/length(x),abs(fft(x)/length(x)));

figure
plot([0:length(x)-1]'/Fs,x)
grid on

% return
%%
cd ('D:\UNI SUBJECTS\Y4S3\FYP2\Pulse Generation');
dlmwrite(['pulse_fs_',num2str(Fs/1e3),'_kHz_fc_',num2str(fc/1e3),'_kHz.txt'],x,'delimiter','\t')

```

Figure 3-11: Code for Signal Generation

Computer device that support the software, National Instruments LABVIEW will be used for first step in signal processing. It is a program for AE feature, signal processing, storage, display and replay. When data is recorded, it can be stored into computer in tdms format.

MATLAB can be used for further signal processing. Time domain data saved in tdms format will be transformed into frequency domain using Fast Fourier Transform (FFT) function included in MATLAB. Both time domain and frequency domain results will be plotted into graph.

### 3.3.6 Experimental Setup

Figure 3.12 shows the design of experimental setup of this study. The first AE sensor will be allocated Xcm away from the artificial defect while the second sensor will be located at Ycm at right side of artificial defect.

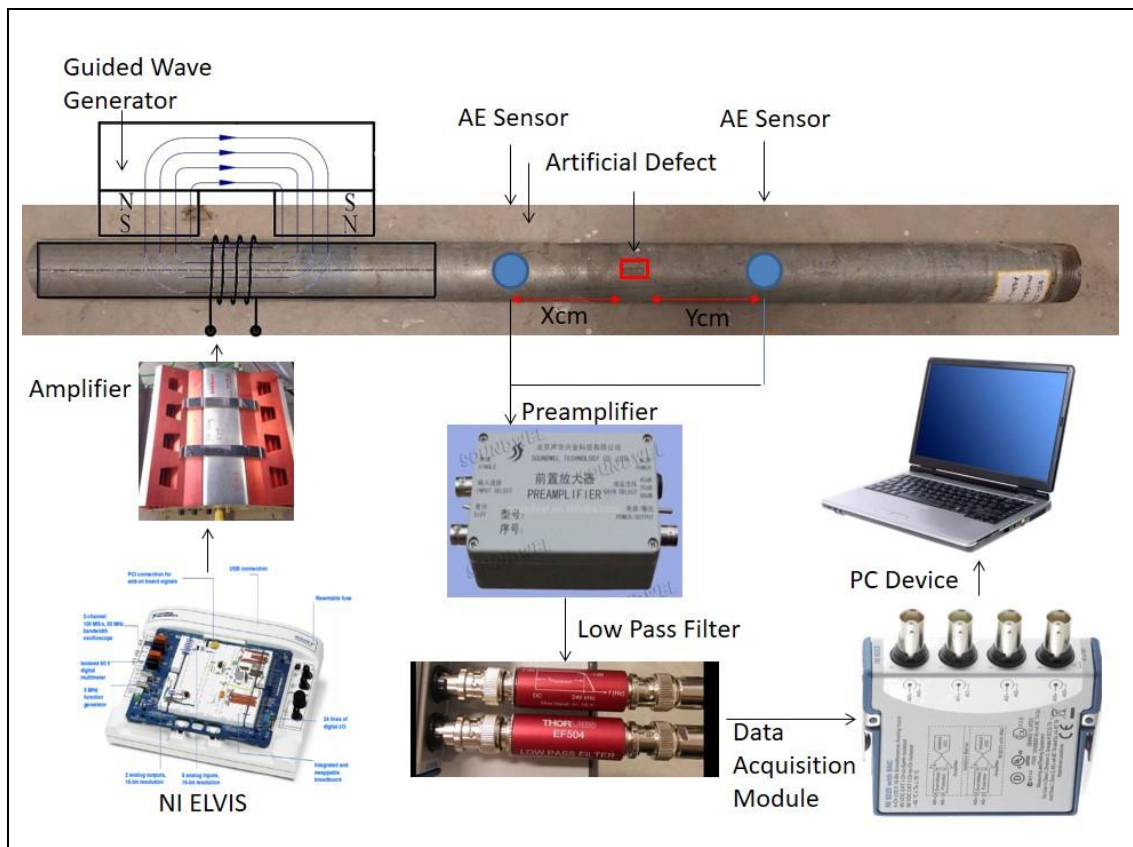


Figure 3-12: Design of Experimental Setup

## CHAPTER 4

### RESULTS AND DISCUSSIONS

#### 4.1 Introduction

In this chapter, the details of test rig and GW signal generator built will be included in first section. The results of generated signal using MATLAB and results of gathered data will be discussed.

#### 4.2 Experimental Setup

Figure below shows the working space and the test rig. The pipe mounted with sensors and magnet is the pipe with 6cm artificial defect while the other pipe is the pipe with 4cm artificial defect.

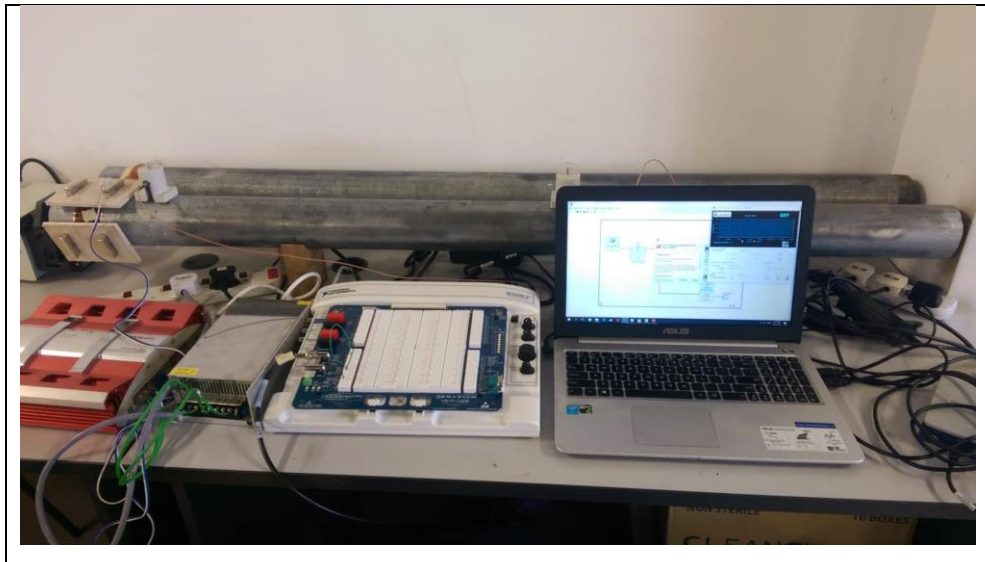


Figure 4-1: Experimental Setup

Another set of data is collected at the pipe located at rooftop of Universiti Tunku Abdul Rahman, Sungai Long.



Figure 4-2: Experimental Setup at Rooftop

Figure 4.3 below shows the model of GW signal generator, the size of the N35 magnets is 50mm x 25mm x 10mm. The angle between each pairs of magnets is  $120^\circ$  to provide a uniform bias magnetic field. Number of turns of wire is 300 turns with resistance of  $9\Omega$ .

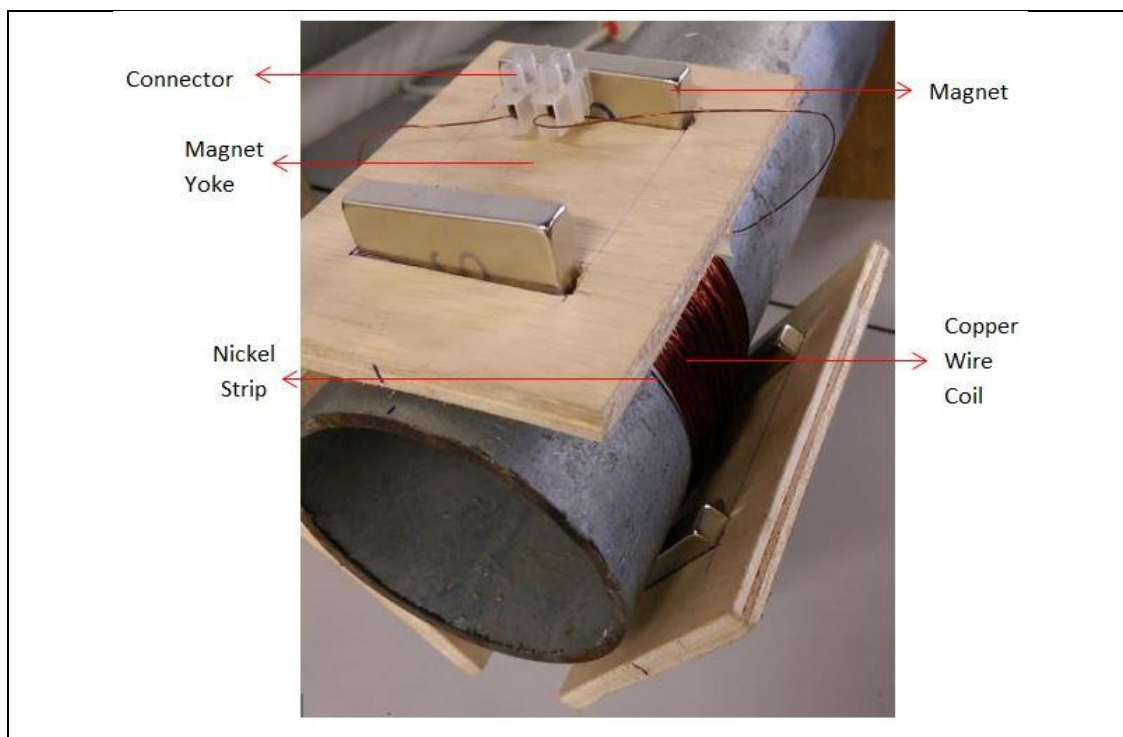


Figure 4-3: GW Signal Generator

### 4.3 Generated Signal

Signal with frequencies of 30kHz, 45kHz, 60kHz, 75kHz were generated in MATLAB. Example of 60 kHz signal is shown in figure below.

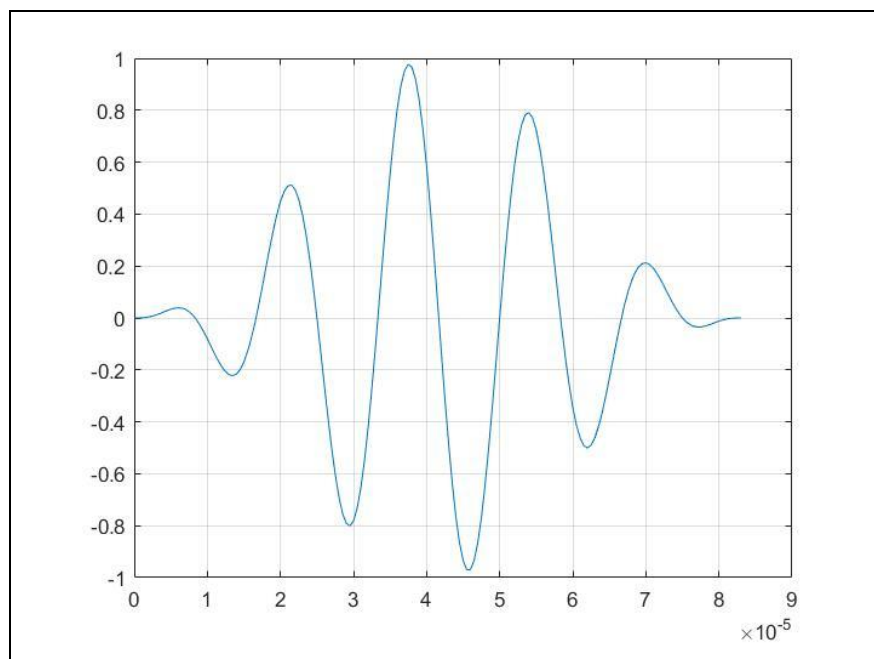


Figure 4-4: Signal with 60 kHz Frequency

### 4.4 User Interface in Data Acquisition

The block diagram and user interface for data acquisition were designed using the software LABVIEW, which are shown in figure below.

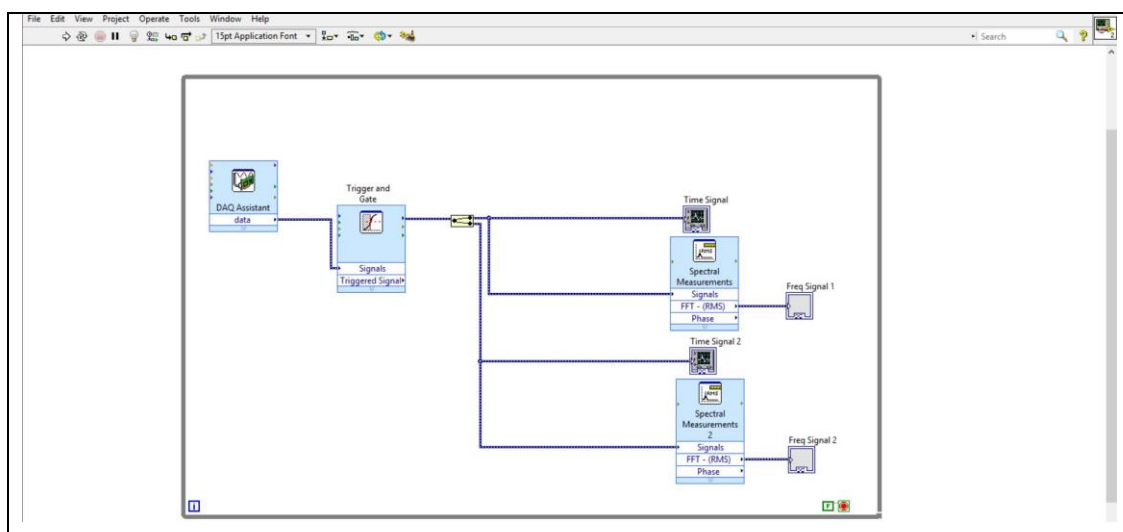


Figure 4-5: Block Diagram in LABVIEW

The 2 graphs at top will show the result in time domain collected by sensor 1 and sensor 2 with time (ms) in X-axis and amplitude in Y-axis. While the 2 graphs at bottom show the result of sensor 1 and sensor 2 in frequency domain with frequency (Hz) in X-axis and amplitude in Y-axis.

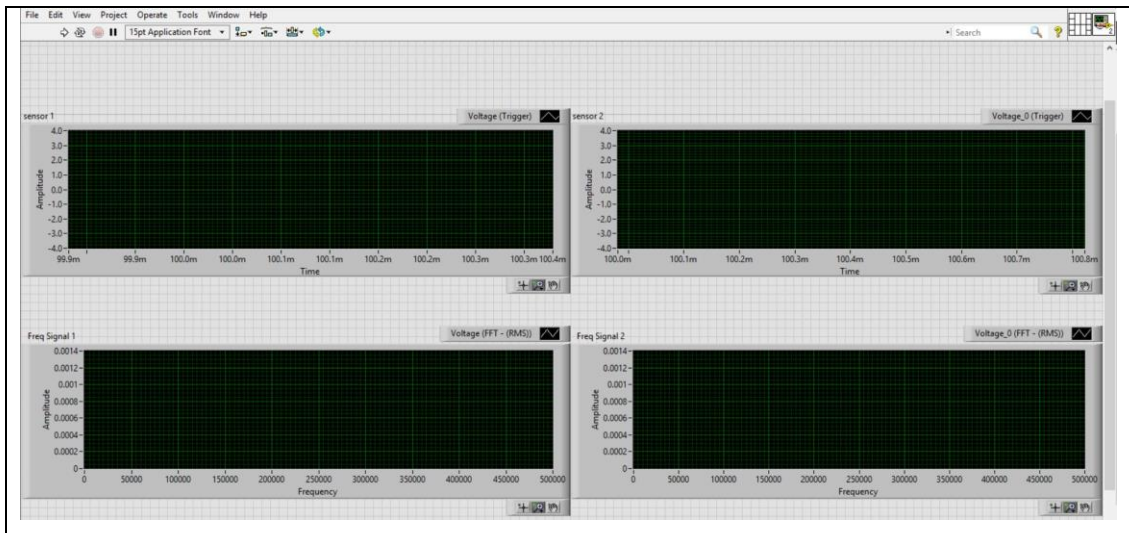


Figure 4-6: User Interface of Data Acquisition

#### 4.5 Results Collected at Pipeline With 6cm Defect.

The first set of results was gathered at the pipeline with 6cm artificial defect. The distance between the sensor 1 and defect is 40cm while 20cm for sensor 2 and defect as shown in figure 4.7. The reason of choosing 40cm as the distance between sensor 1 and sensor 2 is to minimize the interference caused by the reflection of wave signal due to open-end of the pipeline and defect. 4 sets of data were collected with frequency of 30kHz, 45kHz, 60kHz and 70kHz.

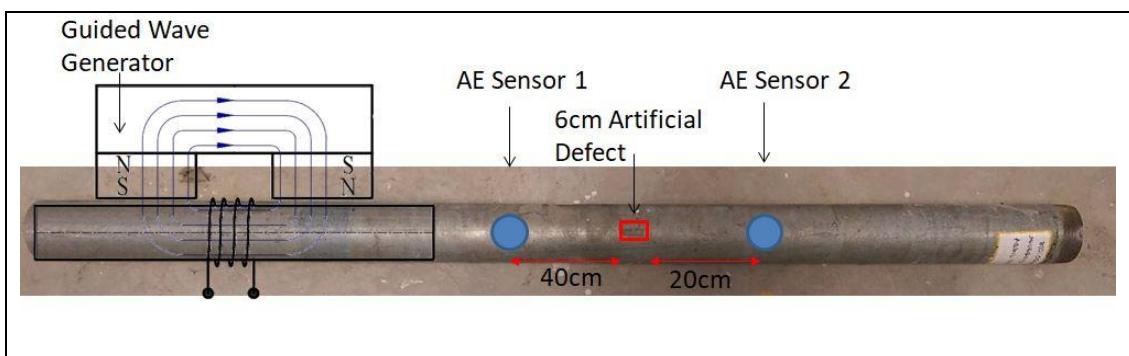


Figure 4-7: Location of Sensors at 6cm Defect Pipeline

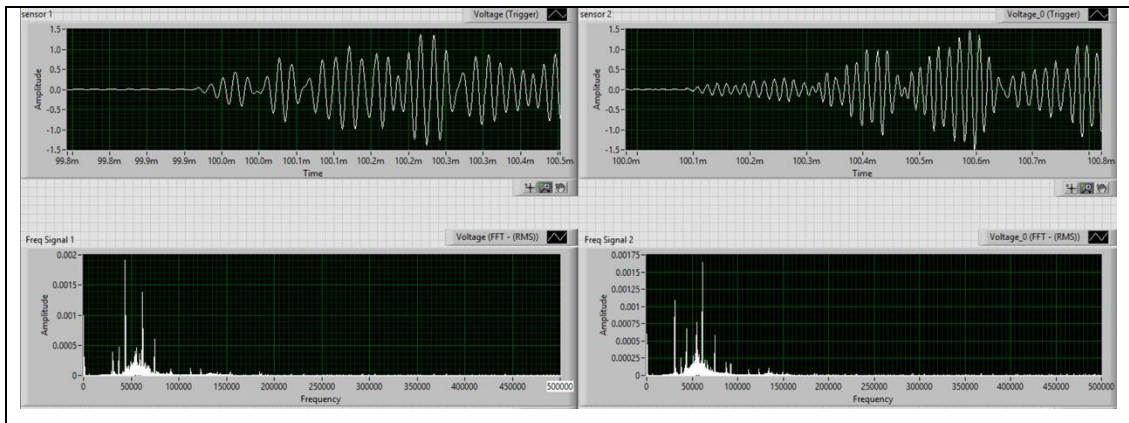


Figure 4-8: Result on 6cm Defect Using 75 kHz Frequency

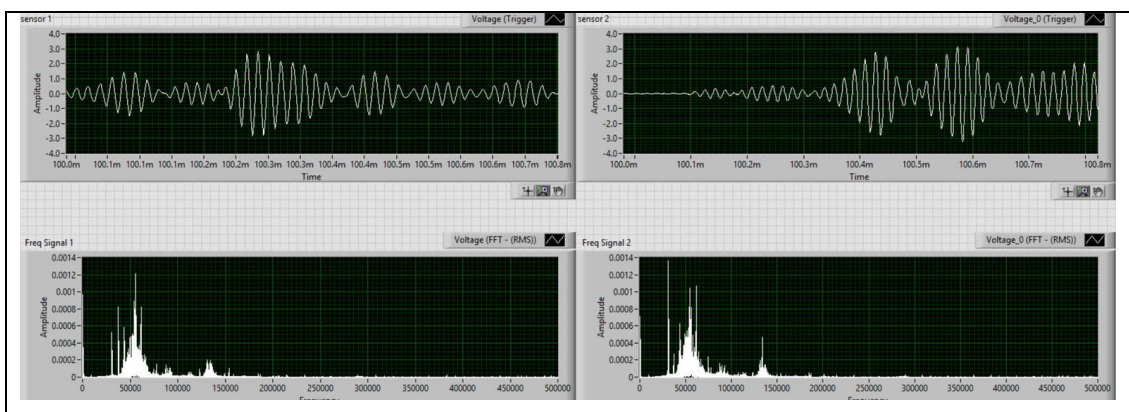


Figure 4-9: Result on 6cm Defect Using 60 kHz Frequency

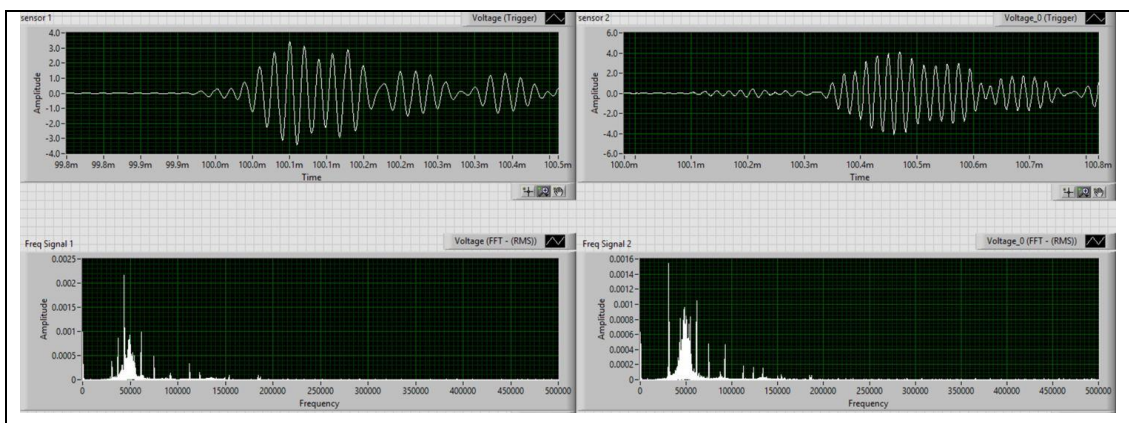


Figure 4-10: Result on 6cm Defect Using 45 kHz Frequency

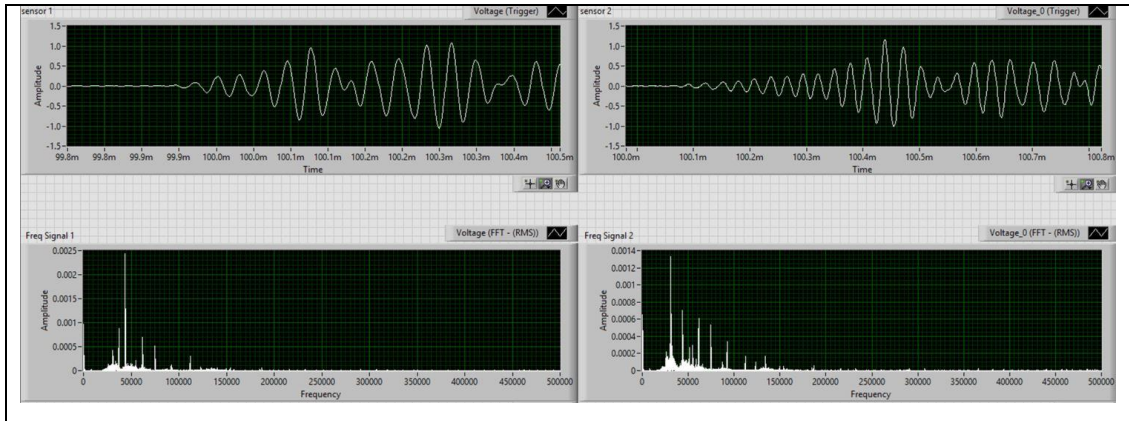


Figure 4-11: Result on 6cm Defect Using 30 kHz Frequency

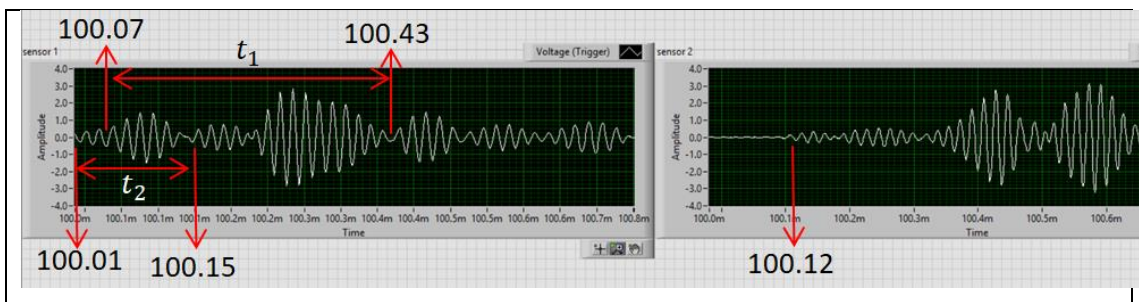


Figure 4-12: Calculation Based on Result of 60 kHz frequency

Calculation is done using result collected with 60 kHz signal.  $t_1$  is the time between the wave  $L(0, 1)$  and its reflection due to the defect;  $t_2$  is the time between the wave  $L(0, 2)$  and its reflection due to the defect. Distance between 2 waves is  $40\text{cm} \times 2 = 80\text{cm}$ .

For  $L(0,1)$ ,

$$t_1 = 100.43 - 100.07 \\ = 0.36\text{ms}$$

$$V_{L(0,1)} = \frac{D}{t_1} = \frac{0.8}{0.00036} \\ = 2222\text{m/s}$$

For  $L(0,2)$ ,

$$t_2 = 100.15 - 100.01 \\ = 0.14\text{ms}$$

$$V_{L(0,2)} = \frac{D}{t_1} = \frac{0.8}{0.00014} \\ = 5714\text{m/s}$$



To further confirm that the first signal obtained is the wave mode with higher speed which is L(0,2), data from sensor 2 is taken into calculation:

*Distance between 2 sensors: 60cm*

*Time different obtain first signal from 2 sensors: 100.12ms – 100.01ms*  
 $= 0.00011\text{ms}$

$$V_{L(0,2)} = \frac{D}{t} = \frac{0.6}{0.00011} = 5454\text{m/s}$$

From the calculations, obtained that the wave velocity is near to the wave velocity of mode L(0,1) and L(0,2) obtained in dispersion curve, refer Figure 4.13.

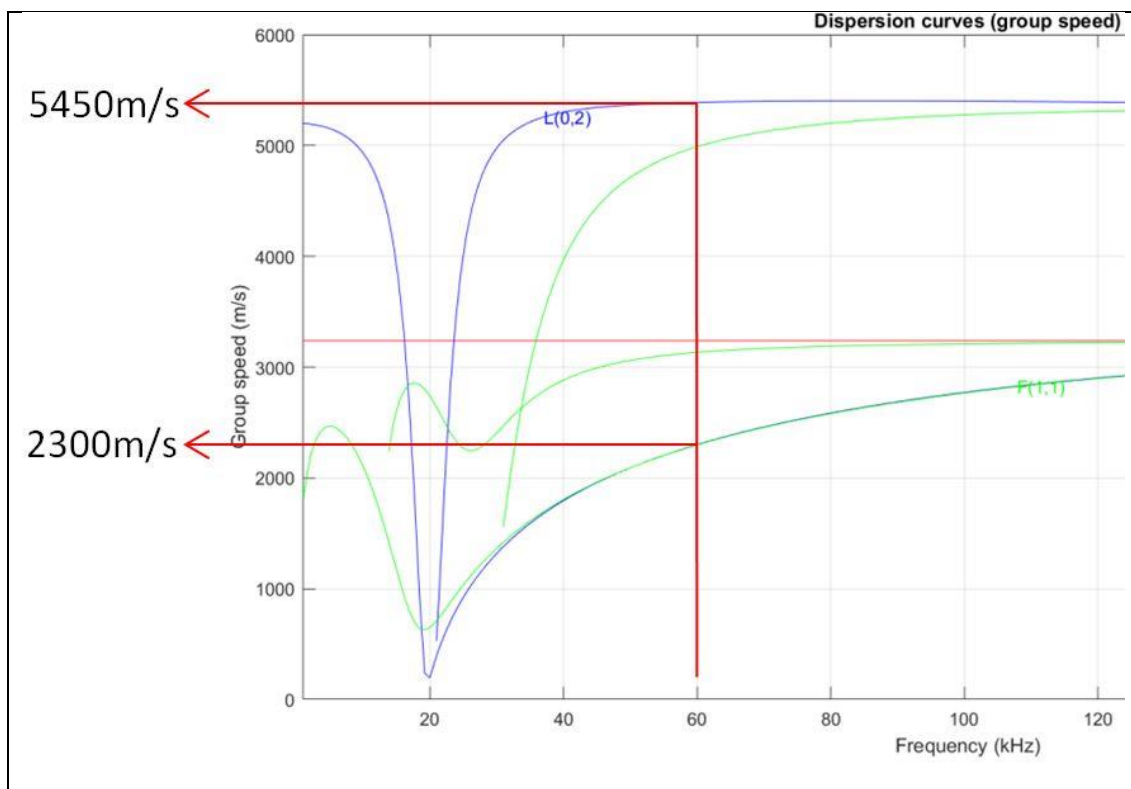


Figure 4-13: Wave Mode Velocity at 60kHz Frequency

#### 4.6 Results Collected at Pipeline With 4cm Defect.

The first set of results was gathered at the pipeline with 6cm artificial defect. The distance between the sensor 1 and defect is 40cm while 20cm for sensor 2 and defect

as shown in figure 4.14. The reason of choosing 40cm as the distance between sensor 1 and sensor 2 is to minimize the interference caused by the reflection of wave signal due to open-end of the pipeline and defect. 3 sets of data were collected with frequency of 45kHz, 60kHz and 70kHz.

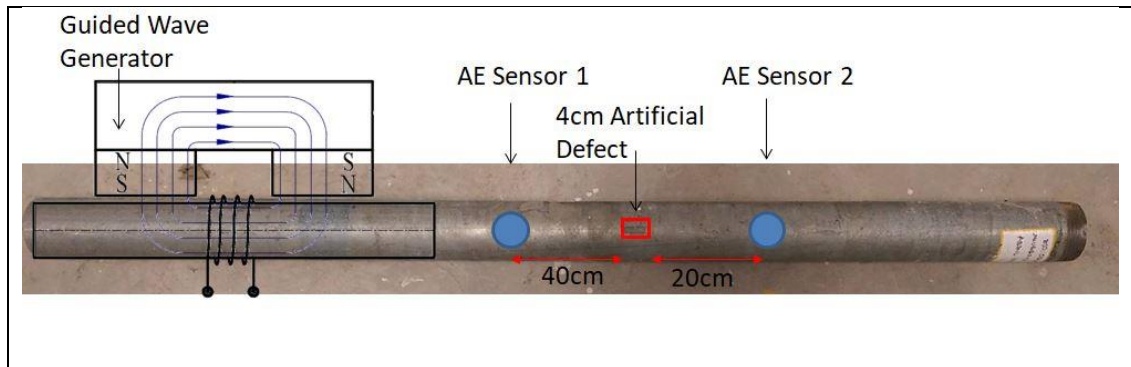


Figure 4-14: Location of Sensors at 4cm Defect Pipeline

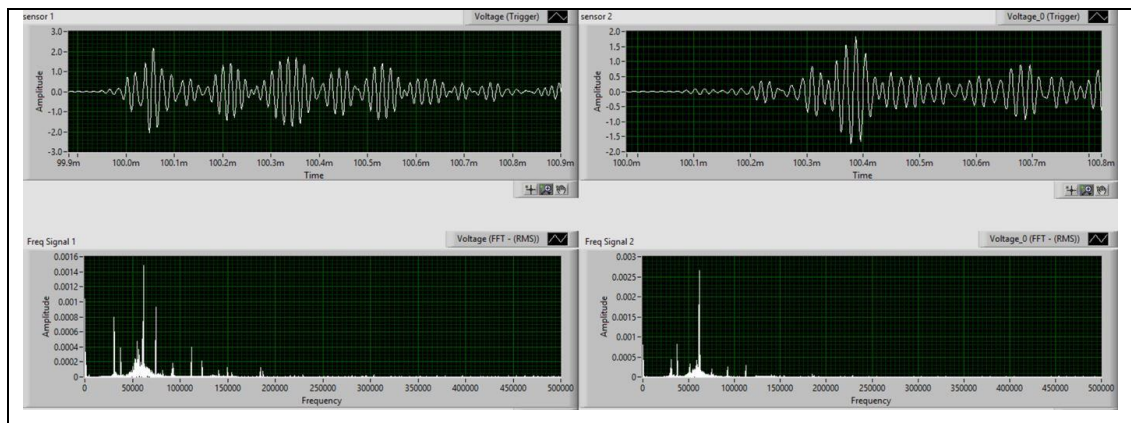


Figure 4-15: Result on 4cm Defect Using 75 kHz Frequency

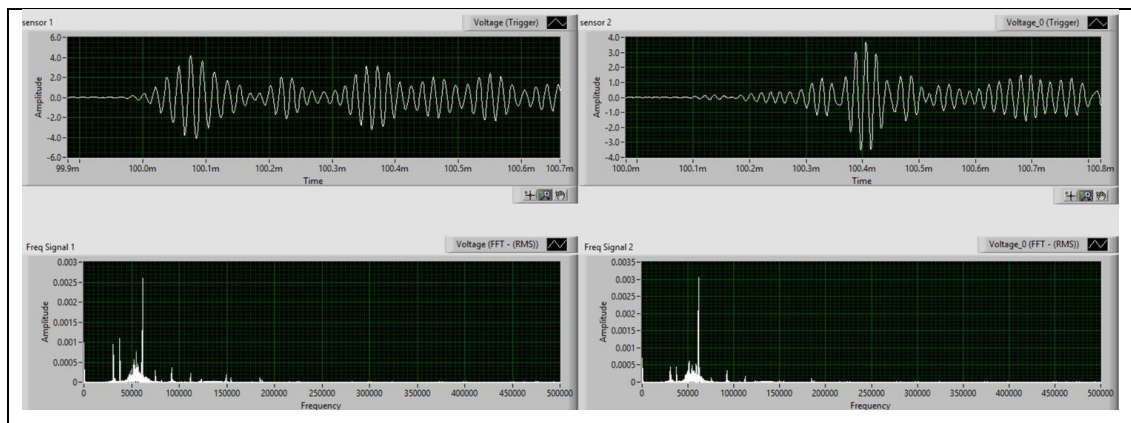


Figure 4-16: Result on 4cm Defect Using 60 kHz Frequency

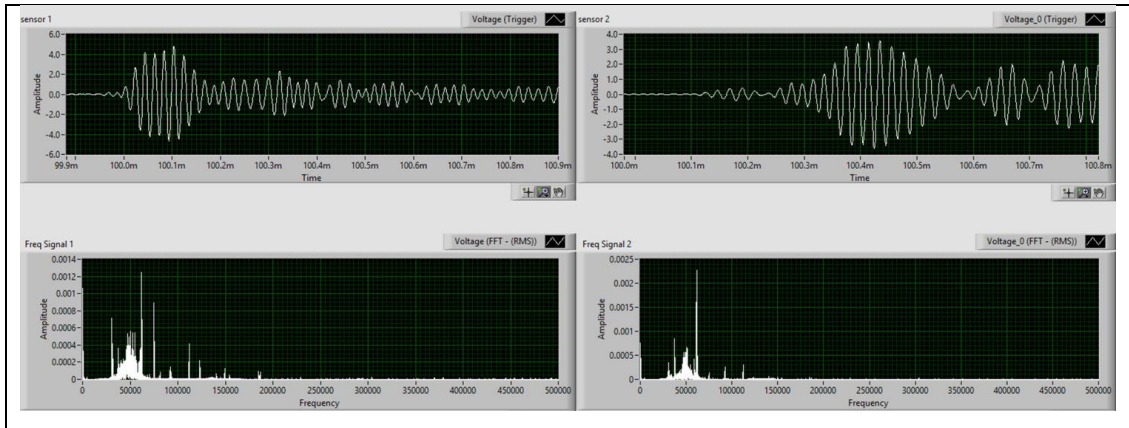


Figure 4-17: Result on 4cm Defect Using 45 kHz Frequency

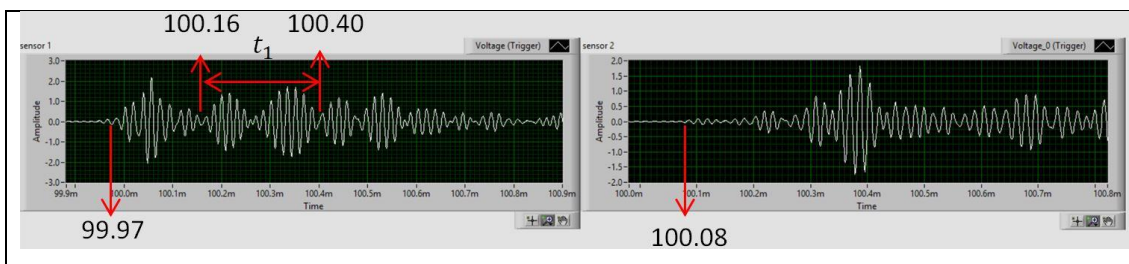


Figure 4-18: Calculation Based on Result of 75 kHz frequency

Calculation is done using result collected with 75 kHz signal.  $t_1$  is the time between the wave  $L(0, 1)$  and its reflection due to the defect. Wave mode  $L(0,2)$  cannot be observed clearly from the data collected from sensor 1 because of the interference with the reflected wave. Wave mode  $L(0,2)$  only can be determined by using the time both sensors detected the first signal.

$$\begin{aligned}
 & \text{For } L(0,1), \\
 & t_1 = 100.40 - 100.016 \\
 & = 0.34ms \\
 & V_{L(0,1)} = \frac{D}{t_1} = \frac{0.8}{0.00034} \\
 & = 2353m/s
 \end{aligned}$$

To further confirm that the first signal obtained is the wave mode with higher speed which is  $L(0,2)$ , data from sensor 2 is taken into calculation:

*Distance between 2 sensors: 60cm*

Time different obtain first signal from 2 sensors: 100.08ms – 100.97ms  
 = 0.00011ms

$$V_{L(0,2)} = \frac{D}{t} = \frac{0.6}{0.00011} = 5454m/s$$

From the calculations, obtained that the wave velocity is near to the wave velocity of mode L(0,1) and L(0,2) obtained in dispersion curve, refer Figure 4.19.

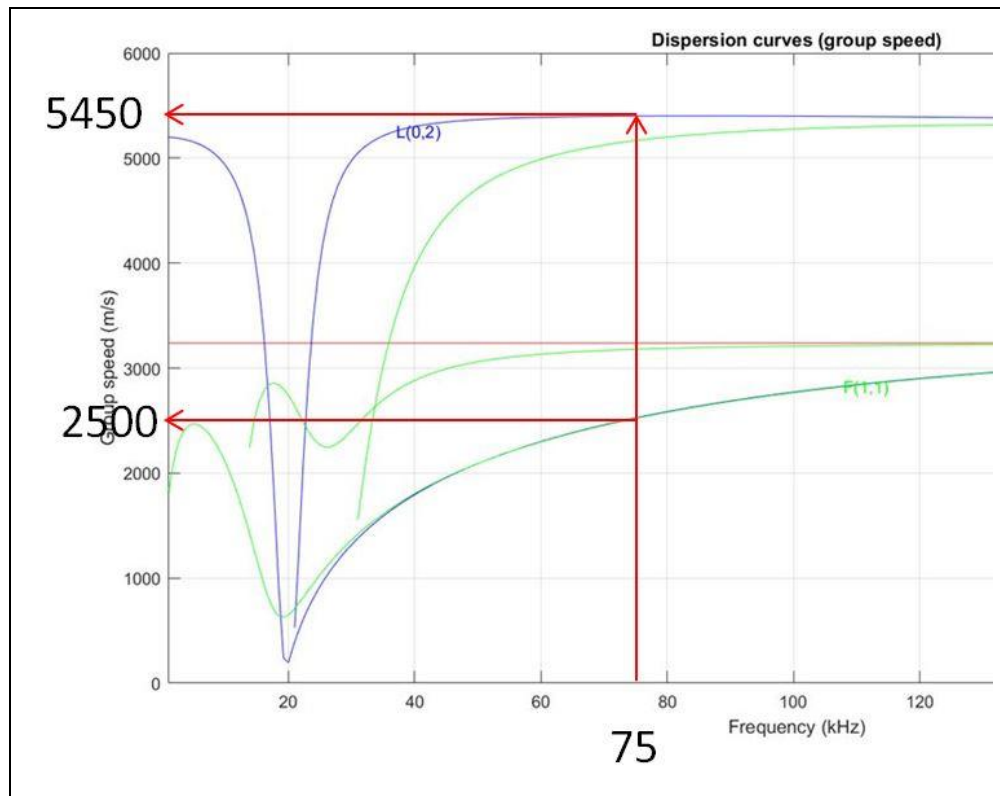


Figure 4-19: Wave Mode Velocity at 75kHz Frequency

#### 4.7 Results Collected at 36m Pipeline

From previous sections, it can be observed that many signal obtained were interfered with reflected signal. This can be caused by the wavelength of the signal was too long due to low frequency. Wavelength can be calculated using the formula:

$$\lambda = \frac{V}{f}$$

Where

$\lambda$	Wavelength;
$V$	Velocity of wave;
$f$	Frequency of wave;

Take 60kHz frequency as example, wavelength of mode L(0,1) and L(0,2) can be calculated using the formula:

$$\begin{aligned}\lambda_{L(0,1)} &= \frac{V_{L(0,1)}}{f} \times 5 \text{ cycles} \\ &= \frac{2300m/s}{60kHz} \times 5 \text{ cycles} \\ &= 0.192m\end{aligned}$$

$$\begin{aligned}\lambda_{L(0,2)} &= \frac{V_{L(0,2)}}{f} \times 5 \text{ cycles} \\ &= \frac{5450m/s}{60kHz} \times 5 \text{ cycles} \\ &= 0.46m\end{aligned}$$

From the calculations, obtained that the wavelength of the 2 longitudinal wave mode L(0,1) and L(0,2) is 0.192m and 0.46m. The length of this wavelength will cause problem of interference between generated signal and reflected signal by defect like corrosion and crack. To further prove that interference of waves will be caused by defects, a set of data was collected at a 36 meter long pipeline.



Figure 4-20: Location of 36m Pipeline



Figure 4-21: Welded spot and Pipeline Holder

In this section, all results were taken using 60kHz frequency. Data were taken with different distance between sensor and GW generator, distance will be mentioned at the caption of the figures below.

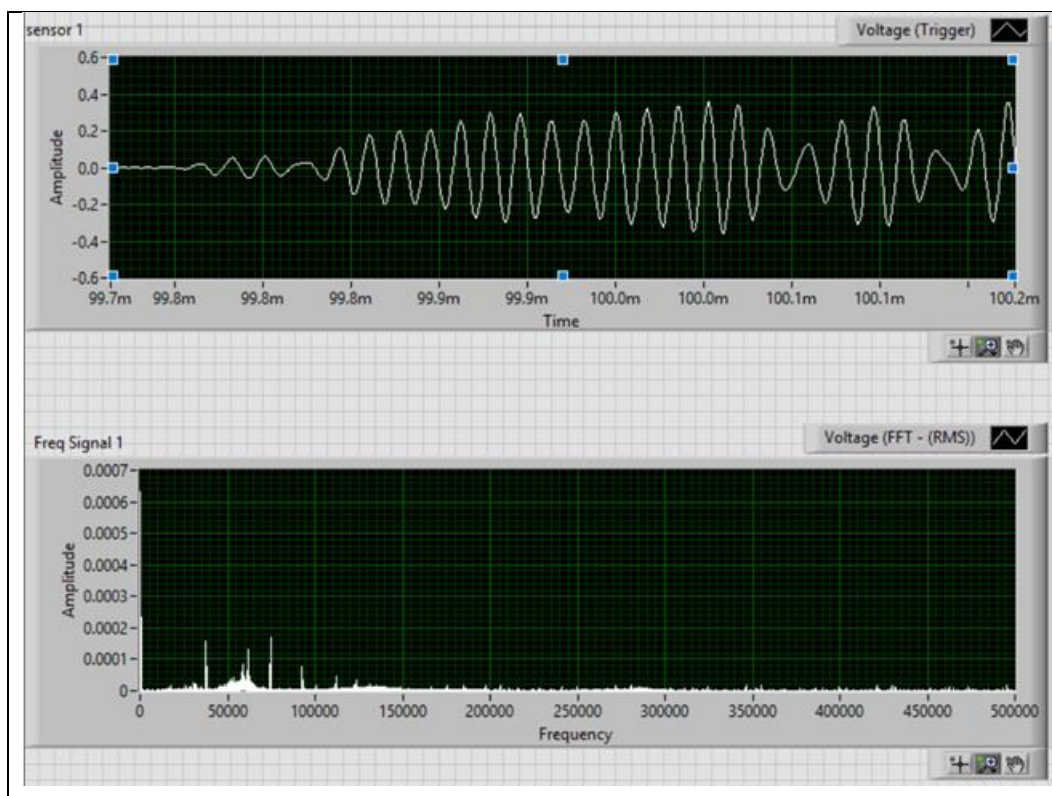


Figure 4-22: Distance between Sensor & Actuator: 60cm

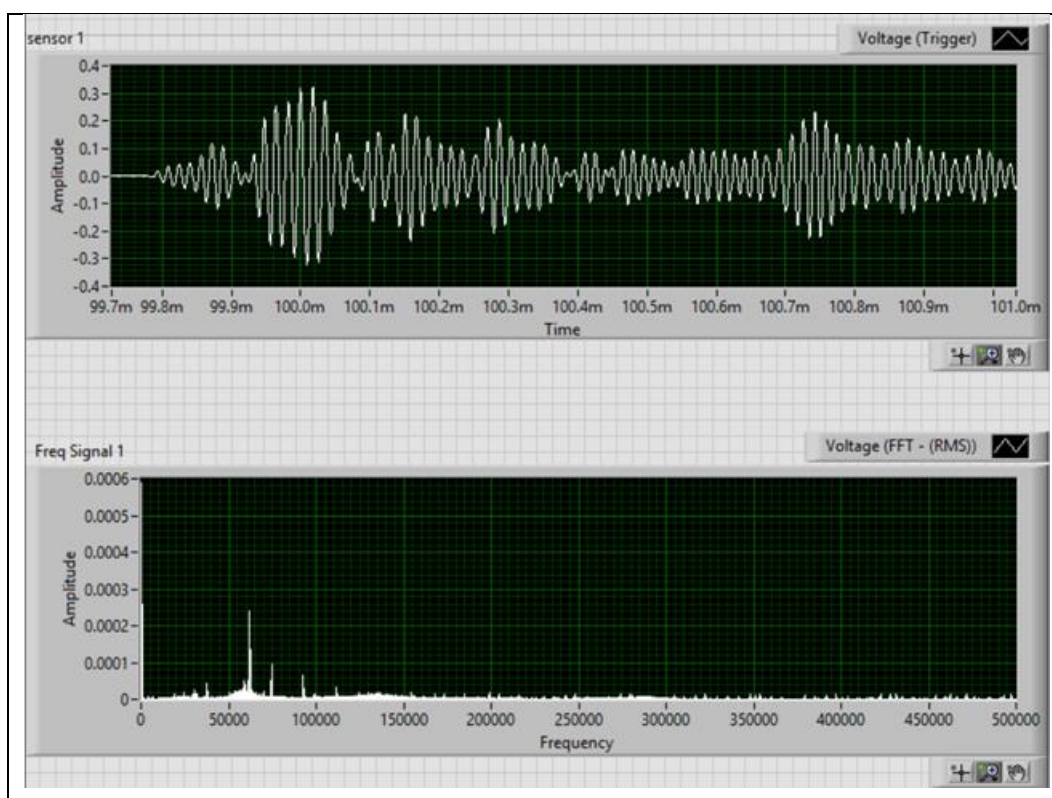


Figure 4-23: Distance between Sensor & Actuator: 40cm

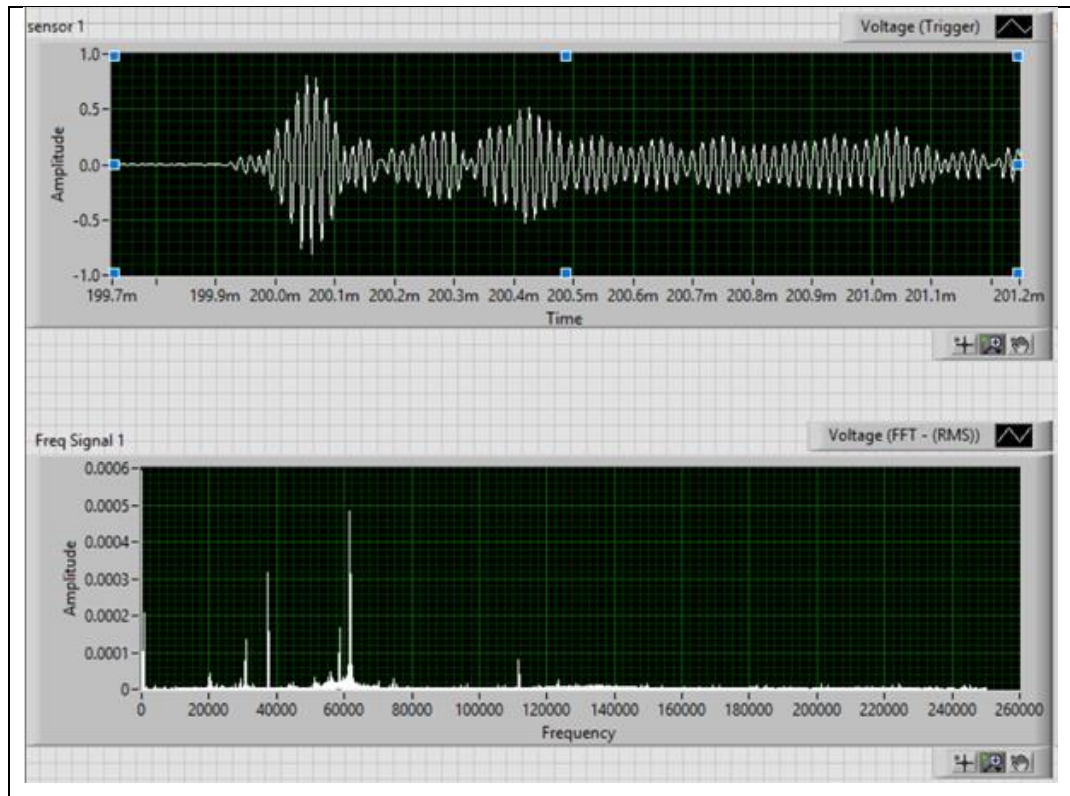


Figure 4-24: Distance between Sensor & Actuator: 20cm

From results obtained above, it can be observed that interference of wave mode  $L(0,1)$  and  $L(0,2)$  occurred. The faster wave mode  $L(0,2)$  was interfered with the slower wave mode  $L(0,1)$ .

In order to observe  $L(0,2)$  clearly from the LABVIEW, the interference of 2 longitudinal wave must be solved, the minimum time and distance of wave mode  $L(0,2)$  required to propagate to overtake wave mode  $L(0,1)$  can be calculated:

$$\begin{aligned}
 \text{Time required} &= \frac{\text{wavelength of } L(0,2)}{V_{L(0,2)} - V_{L(0,1)}} \\
 &= \frac{0.46\text{m}}{(5450 - 2300)\text{m/s}} \\
 &= 1.46 \times 10^{-4} \text{s}
 \end{aligned}$$

$$\begin{aligned}
 \text{Distance required} &= V_{L(0,2)} \times \text{Time required} \\
 &= 5450\text{m/s} \times 1.46 \times 10^{-4} \text{s} \\
 &= 0.7957\text{m} \cong 0.8\text{m}
 \end{aligned}$$



From the calculation above, obtained that minimum distance required for wave mode  $L(0,2)$  to overtake wave mode  $L(0,1)$  so that the interference of these 2 generated wave can be solved is 0.8m. Few set of results were obtained after reposition the sensor away from the actuator at least 0.8m.

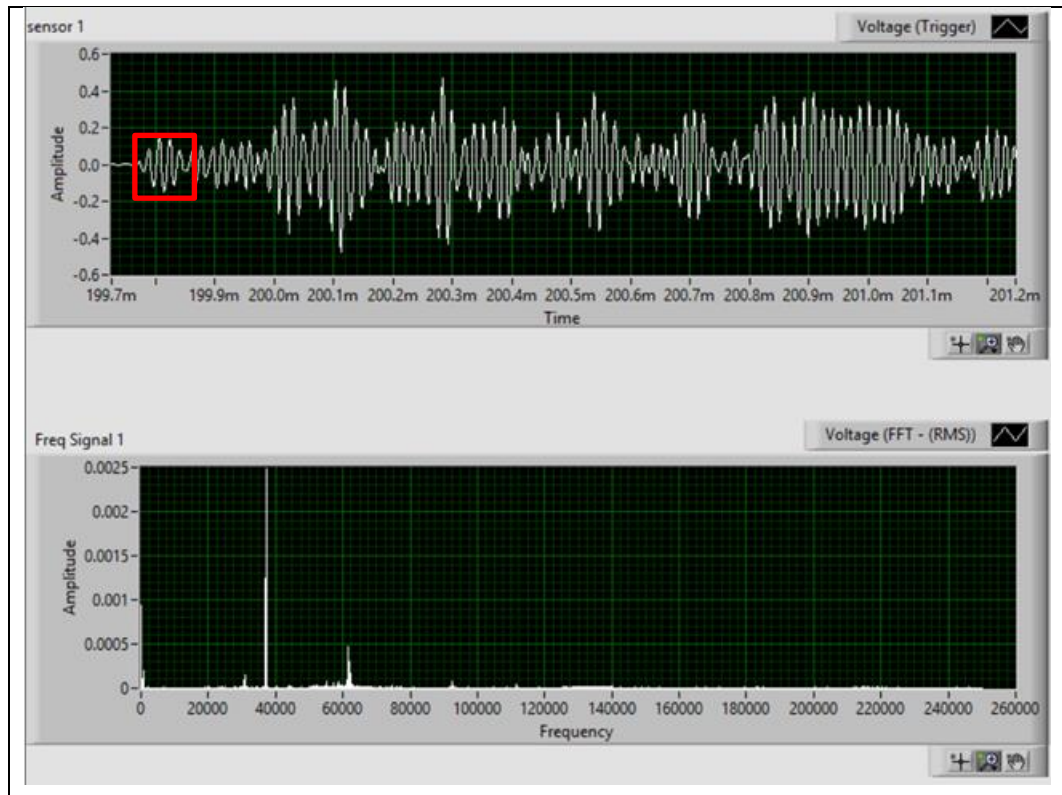


Figure 4-25: Distance between Sensor & Actuator: 90cm

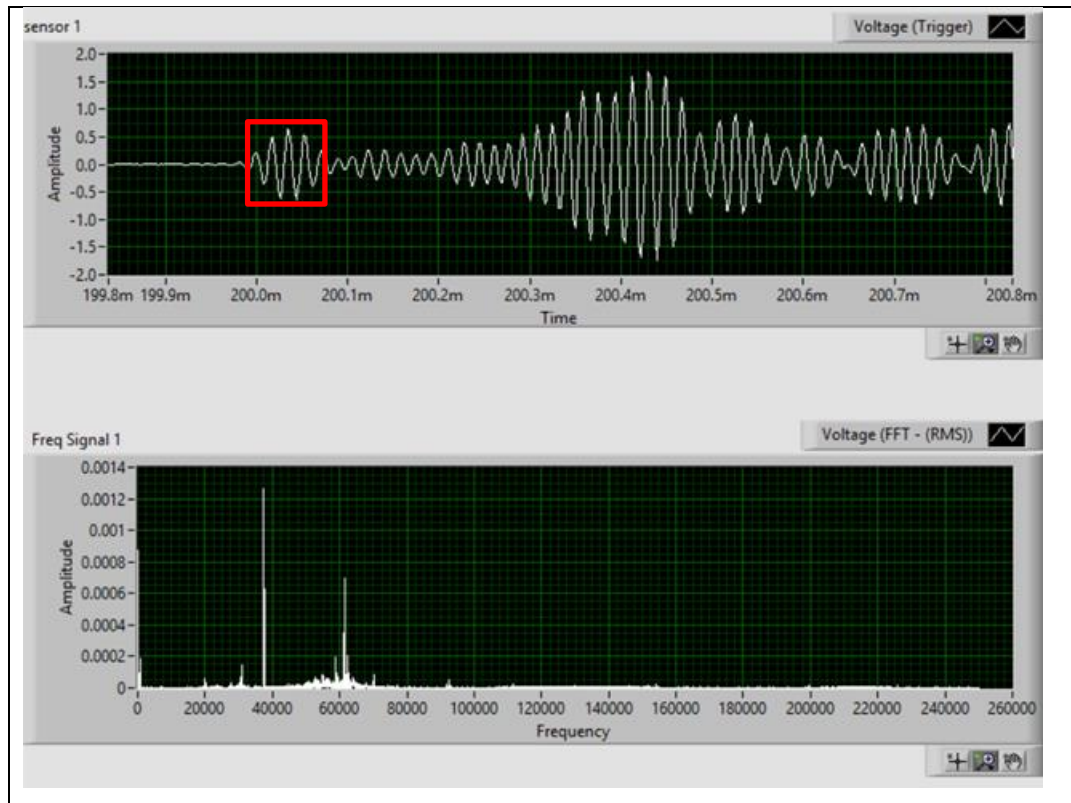


Figure 4-26: Distance between Sensor & Actuator: 110cm

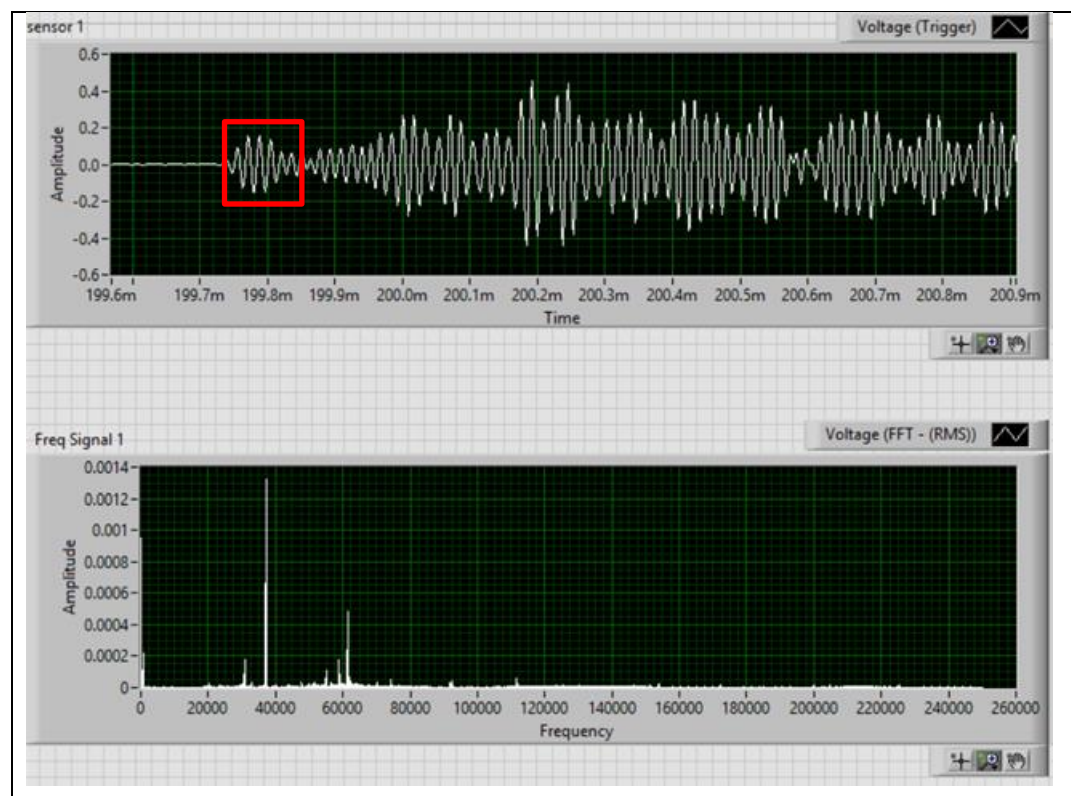


Figure 4-27: Distance between Sensor & Actuator: 130cm

The distances between the sensor and the actuator were 90cm, 110cm and 130cm. By comparing results obtained before and after calculation of required distance, the faster wave mode,  $L(0,2)$  can be obtained clearly from the graphs.

#### **4.8 Summary**

From the results, obtained that the velocity of longitudinal waves generated is similar with the velocity of waves obtained from dispersion curve. This proved that the mode of the generated signal is able to controlled using magnet. This also further proves that the velocity of the wave generated can be controlled by controlling the frequency of the wave using MATLAB.

From the calculation, we can obtain that the location of the defect can be determine by measuring the time between generated signal and reflected signal and velocity of the wave.

From this study, student also found that 1.5m long pipeline is not suitable for this study. The lower the frequency, the longer the wavelength, in this study, maximum 75k Hz of frequency is used because of the limitation of sensors. This had caused the interference of generated wave and reflected wave. Results are harder to be analysed when interference happens. Recommendations for this issue will be discussed in next section.

From the results, another problem encounter is background noise. Background noise is the unwanted signal caused by the environment. In this study, background noise may be caused by electronics like laptop, power supply, pump, compressor etc. From the frequency domain results, observed that the frequency obtained is not only consist of the frequency generated. After comparing the all results, the unwanted signal obtained can be determined are background noises. These noises may cause false defect detection. To solve this problem, a strong programming skill in MATLAB is required. Noise cancellation technique like cross-correlation, wavelet transform in MATLAB for noise cancellation is highly recommended in this study to make this project better.

## CHAPTER 5

### CONCLUSIONS AND RECOMMENDATIONS

#### 5.1 Conclusions

The aims and objectives of this project are achieved. In section 4.2, the construction of GW actuator was introduced and its function is good to generate signal for a 1.5 long pipe. In section 4.5, the defect of the pipeline can be detected by observing the reflection of both wave mode  $L(0,1)$  and  $L(0,2)$ . While in section 4.6, the defect only can be detected by observing the wave mode  $L(0,1)$  due the interference of both generated wave mode. In section 4.7, the minimum required propagate distance of 0.8m was obtained by calculation to solve the problem of interference of both longitudinal wave mode.

In conclusion, a GW actuator is designed and built in this study, the location of defect also can be determined using GW actuator by controlling the velocity of wave generated and measure the time between generated signal and reflected signal. From the results, student also found that the 1.5m long pipe is not suitable for the test rig due to the problem of interference. A longer pipe such as 6m may contribute a better result since the reflected wave can be determined more easily.

However, there are still many improvements and works can be done to obtain a more accurate result.

#### 5.2 Recommendations for Future Work

The lengthy of wavelength is a disadvantage of low frequency signal, there are 2 recommendations to tackle this problem. In my project, I use 1.5m pipe as test rig, it is better to use a longer pipe without welded if want to detect an artificial defect because welded spot will cause reflection. Another recommendation is use a sensor that has a higher pickup frequency. From dispersion curve, obtained that the velocity of waves is less dispersive in high frequency range. From the wavelength formula, also knew that the wavelength is inversely proportional to frequency, the higher the frequency the shorter the wavelength.

Although high frequency has a shorter wavelength, it also has a drawback of short propagating distance. A recommendation for this drawback is use iron cobalt to

replace nickel as the magnetostrictive transducer, as mentioned in Chapter 2 that iron cobalt alloy has a better result for a magnetostrictive transducer. It has a higher sensitivity and power output for detection and long range inspection.

From the results, we also can observed that there are many background noises that caused by electronics like computer, power supply. A noise cancellation technique also can be included in future work.

Last but not least, to follow the trend of industry 4.0 and 5G networking era, online inspection technique also can be included in future work. With this, inspectors do not have to work on site to acquire data.

## REFERENCES

- Alleyne, D. N., Vogt, T. and Cawley, P. (2009) 'The choice of torsional or longitudinal excitation in guided wave pipe inspection', *Insight: Non-Destructive Testing and Condition Monitoring*, 51(7), pp. 373–377. doi: 10.1784/insi.2009.51.7.373.
- Bertoncini, F. *et al.* (2016) 'Overview and Experimental Evaluation of Magnetostrictive Transducers for Guided Wave Inspection', *Journal of Intelligent Material Systems and Structures*, (SEPTEMBER 2012). Available at: <http://www.researchgate.net/publication/240600701>.
- Chimenti, D. E. (2014) 'Review of air-coupled ultrasonic materials characterization', *Ultrasonics*. Elsevier B.V., 54(7), pp. 1804–1816. doi: 10.1016/j.ultras.2014.02.006.
- FT Calkins (2006) 'Overview of Magnetostrictive Sensor Technology', 00(1), pp. 1–14. doi: 10.1177/1045389X0.
- Furusawa, A., Kojima, F. and Morikawa, A. (2015) 'Mode control of guided wave in magnetic hollow cylinder using electromagnetic acoustic transducer array', *Nuclear Engineering and Technology*. Elsevier B.V., 47(2), pp. 196–203. doi: 10.1016/j.net.2014.12.007.
- Joule, J. P. (1847) 'XVII. On the effects of magnetism upon the dimensions of iron and steel bars', *The London, Edinburgh, and Dublin Philosophical Magazine and Journal of Science*, 30(199), pp. 76–87. doi: 10.1080/14786444708645656.
- Khaligh, A., Zeng, P. and Zheng, C. (2010) 'Kinetic Energy Harvesting Using Piezoelectric and Electromagnetic Technologies #x2014;State of the Art', *Industrial Electronics, IEEE Transactions on*, 57(3), pp. 850–860. doi: 10.1109/TIE.2009.2024652.
- Kim, Y. Y. *et al.* (2005) 'Torsional wave experiments with a new magnetostrictive transducer configuration', *The Journal of the Acoustical Society of America*, 117(6), pp. 3459–3468. doi: 10.1121/1.1904304.
- Kim, Y. Y. and Kwon, Y. E. (2015) 'Review of magnetostrictive patch transducers and applications in ultrasonic nondestructive testing of waveguides', *Ultrasonics*. Elsevier B.V., 62, pp. 3–19. doi: 10.1016/j.ultras.2015.05.015.
- Liu, Z. *et al.* (2010) 'Configuration optimization of magnetostrictive transducers for longitudinal guided wave inspection in seven-wire steel strands', *NDT and E International*. Elsevier, 43(6), pp. 484–492. doi: 10.1016/j.ndteint.2010.05.003.
- Luo, M. *et al.* (2018) 'Development of a Novel Guided Wave Generation System

Using a Giant Magnetostrictive Actuator for Nondestructive Evaluation', *Sensors*, 18(3), p. 779. doi: 10.3390/s18030779.

Myers, H. P. (1997) *Introductory Solid State Physics*. 2nd edn.

Panda, A. K. *et al.* (2012) 'Generation and detection of guided waves in a defective pipe using rapidly quenched magnetostrictive ribbons', *Smart Materials and Structures*, 21(4). doi: 10.1088/0964-1726/21/4/045015.

Paper, T. and Vinogradov, S. A. (2009) 'Magnetostrictive Transducer for Torsional Guided Waves in Pipes and Plates', (March), pp. 333–341.

Schaal, C. *et al.* (2014) 'Crack Detection in Multi-Wire Cables Using Guided Ultrasonic Waves To cite this version : HAL Id : hal-01022061'.

Tatarinov, A. *et al.* (2018) 'Non-destructive Testing and Repair of Pipelines', pp. 15–30. doi: 10.1007/978-3-319-56579-8.

Vinogradov, S. A. and Leonard, J. (2017) 'Development of Magnetostrictive Sensor Technology for', (6), p. 221.

Wang, C. *et al.* (2016) 'Guided wave mode dispersion of transient acoustic emission on copper pipes - Its visualisation and application to source location', *Mechanical Systems and Signal Processing*. Elsevier, 70–71, pp. 881–890. doi: 10.1016/j.ymssp.2015.09.013.

Zhang, D. *et al.* (2014) 'A Magnetostrictive Guided-Wave Nondestructive', 63(12), pp. 3058–3067.